Geophysical Investigations of the Pensacola Mountains and Adjacent Glacierized Areas of Antarctica

By JOHN C. BEHRENDT, JOHN R. HENDERSON, LAURENT MEISTER, *and* WILLIAM L. RAMBO

GEOLOGICAL SURVEY PROFESSIONAL PAPER 844

Aeromagnetic, gravity, and seismic reflection data allow extension of known geology beneath area covered by ice

UNITED STATES GOVERNMENT PRINTING OFFICE, WASHINGTON : 1974

UNITED STATES DEPARTMENT OF THE INTERIOR

ROGERS C. B. MORTON, *Secretary*

GEOLOGICAL SURVEY

V. E. McKelvey, *Director*

Library of Congress catalog-card No. 74-600032

For sale by the Superintendent of Documents, U.S. Government Printing Office
Washington, D.C. 20402 – Price $2.05 (paper cover)
Stock Number 2401-02499

CONTENTS

	Page
Abstract	1
Introduction	1
Glacial and bedrock physiography	2
Summary of geology	3
Precambrian and Paleozoic rocks	3
Dufek intrusion	5
Latest tectonic activity	6
Geophysical investigations	6
Gravity survey	6
Magnetic survey	7
Seismic reflection measurements	8
Geophysical results	10
Gravity	10
Geophysical results — Continued	
Gravity — Continued	
Neptune and Patuxent Ranges	10
Dufek intrusion	12
Crustal structure	14
Isostasy	15
Magnetic results	15
Dufek intrusion	15
Neptune and Patuxent Ranges	20
Other magnetic anomalies	21
Discussion	21
Summary and conclusions	23
References	23

ILLUSTRATIONS

			Page
PLATE	1.	Bouguer anomaly and generalized geologic map of the Pensacola Mountains area, Antarctica	In pocket
	2.	Aeromagnetic maps of the Pensacola Mountains area, Antarctica	In pocket
FIGURE	1.	Index map of Antarctica	1
	2.	Snow-surface-elevation map	3
	3.	Bedrock-elevation map	4
	4.	Composite stratigraphic section	5
	5.	Diagram showing variation in mafic index with height in the Dufek intrusion	6
	6.	Diagram showing volume percentage of opaque minerals compared with magnetic susceptibility and remanent magnetization in the Dufek intrusion	7
	7.	Reflection seismograms for seismic station 2	9
	8.	Reflection seismogram for seismic station 26	10
	9.	Surface- and bedrock-elevation and free-air gravity-anomaly profiles	11
	10.	Free-air-anomaly map	12
	11.	Bouguer anomaly profile and theoretical crustal models	13
	12.	Graph showing Bouguer anomalies compared with elevation	14
	13.	Map showing prior magnetic data	16
	14.	Magnetic profile along line 11	17
	15.	Magnetic profile along line 18	17
	16.	Magnetic profile along line 26	18
	17.	Upward continuation of magnetic profile along line 11	20
	18.	Map showing reconstruction of Gondwanaland	22

TABLES

			Page
TABLE	1.	Seismic reflection stations in Pensacola Mountains area, 1965–66	8
	2.	Data from gravity reduction program, Camp Neptune, Pensacola Mountains	26

GEOPHYSICAL INVESTIGATIONS OF THE PENSACOLA MOUNTAINS AND ADJACENT GLACIERIZED AREAS OF ANTARCTICA

By JOHN C. BEHRENDT, JOHN R. HENDERSON, LAURENT MEISTER,[1] and WILLIAM L. RAMBO

ABSTRACT

Aeromagnetic, gravity, and seismic reflection measurements in the Pensacola Mountains area of Antarctica have allowed extension of the known geology beneath areas covered by thick ice. A broad regional Bouguer anomaly has gradients parallel to the northwest edge of the Pensacola Mountains block. Bouguer anomaly values decrease from 82 to −90 mgal across this transition from West Antarctica to East Antarctica. Theoretical profiles fitted to the gravity data indicate either an abnormally thin crust on the West Antarctica side or a normal crust on the West Antarctica side and a steep steplike transition from West Antarctica to East Antarctica that suggests a fault extending from the crust-mantle boundary to near the surface in the vicinity of the Schmidt Hills. Gravity, magnetic, and seismic data suggest a thick section of low-velocity, low-density, nonmagnetic, presumably sedimentary rock beneath the ice northwest of the Pensacola Mountains.

A least-squares regression of the Bouguer anomalies compared with elevation in the Pensacola Mountains area suggests that the amplitude of the gravity anomaly associated with the Dufek layered gabbroic intrusion is about 85 mgal, corresponding to about 8.8- to 6.2-km thickness for the intrusion, assuming reasonable density contrasts. Magnetic anomalies approaching 2,000 gammas amplitude are associated with the intrusion. The decrease in amplitudes of one to two orders of magnitude from the northern Forrestal Range to the southern Dufek Massif is consistent with measured magnetic properties (including normal and reversed remanent magnetization); this interpretation is supported by theoretical magnetic models. The models suggest a 4-km fault across the front of the Dufek Massif, down to the northwest. Models fitted to 100- to 200-gamma anomalies over the southern Dufek Massif require a basal section 1−2 km thick of higher magnetization than that measured from rocks in the lowest exposed part of the section, or infinitely thick bodies of the low magnetization actually observed. The first hypothesis is most reasonable and suggests a possible basal ultramafic layer.

Magnetic and gravity data suggest an extension of the Dufek intrusion beneath the ice. The magnetic data indicate a minimum areal extent of about 24,000 km², and gravity data outside the magnetic survey suggest an additional 10,000 km², giving a total minimum estimate of 34,000 km², at least half the area of the Bushveld complex in Africa. Other magnetic data suggest a possible continuation of the Dufek intrusion as far north as Berkner Island.

Several magnetic and gravity anomalies of limited areal extent are associated with small-scale geologic sources within the Pensacola Mountains and beneath the ice sheet. Precambrian diabase intrusions in the Schmidt Hills area are inferred to be the sources of 50-gamma magnetic anomalies. A −200-gamma magnetic anomaly and a positive Bouguer anomaly in the Weber Ridge area at the north end of the Patuxent Range are interpreted as caused by a mafic intrusion. A negative anomaly of at least −30-mgal lies over the granite of Median Snowfield and Beacon (?) sedimentary rocks in the Washington Escarpment area relative to the Patuxent Formation in the Neptune Range.

The free-air-anomaly data and the Bouguer anomaly−elevation regression calculation suggest that the area is in regional isostatic equilibrium.

[1]Geophysical Service International.

INTRODUCTION

In this report we discuss our geophysical work in the Pensacola Mountains and surrounding ice-covered areas of Antarctica and our interpretations of these data as related to the geology. Figure 1 shows the general area of study. The Pensacola Mountains are part of the more than 3,000-km-long Transantarctic Mountains system and were discovered on a U.S. Navy flight from McMurdo Sound in 1956. The Filchner Ice Shelf Traverse in 1957 (Neuburg and others, 1959) crossed the Dufek Massif at the north end of the Pensacola Mountains after crossing the Filchner Ice Shelf from Ellsworth Station, and rocks were collected in the Dufek Massif. Various reports on the work of this traverse (for example, Behrendt, 1962a; Thiel and others, 1958; Neuburg and others, 1959; and Aughenbaugh, 1961) discussed scientific results. Neuburg, Thiel, Walker, Behrendt, and Aughenbaugh (1959) and Aughenbaugh (1961) first reported the existence of the Dufek intrusion,

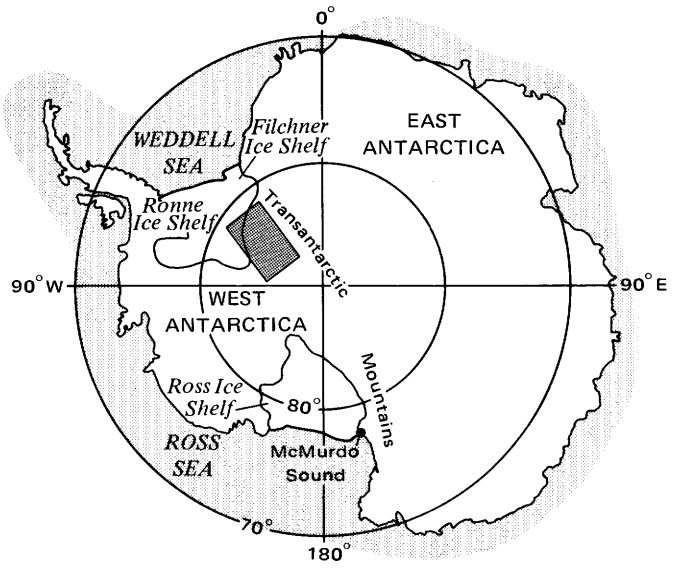

FIGURE 1. — Index map of Antarctica, showing location of Pensacola Mountains area (dark shaded rectangle).

which we will discuss at some length in this report. They observed that the Dufek Massif was composed of layered gabbro, and they suggested that a large igneous intrusion had developed layering through segregation during cooling of magma. Ford and Boyd's (1968) later work supports this interpretation.

Detailed geologic investigations of the Pensacola Mountains were carried out during the 1962–64 field seasons (Schmidt and others, 1964, 1965). Geophysical investigations in the area started in 1957–58 with seismic reflection soundings and gravity and magnetic measurements on the Ronne Ice Shelf (Thiel and others, 1958; Behrendt, 1962a). During the 1963–64 season, Manfred Hochstein, of the University of Wisconsin, led an oversnow traverse into the area west of the Pensacola Mountains and made similar geophysical measurements and seismic refraction measurements of bedrock velocity. Also during the 1963–64 season, flights into the Dufek Massif and Forrestal Range of the Pensacola Mountains (Behrendt, 1964) first recorded the high-amplitude magnetic anomalies associated with these ranges. The Forrestal Range had not been visited on the ground prior to that time, so on the basis of the magnetic anomalies it was assumed to be of gabbroic composition similar to that of the Dufek Massif.

The results of this early work were encouraging and indicated the need for further study. Therefore, during the 1965–66 season, a large-scale scientific effort was made in the Pensacola Mountains area (Huffman and Schmidt, 1966). Trimetrogon aerial photographs that were taken on cooperative flights by the U.S. Navy and the U.S. Geological Survey previous to the 1965–66 season allowed compilation of preliminary maps, and one of the objectives of the 1965–66 party was to establish topographic control sufficient for compilation of 1 : 250,000-scale topographic maps. The scientific party conducted eight integrated projects — geological, aeromagnetic, gravity, seismic, geodetic, paleobotanic, paleosedimentological, and entomological observations. U.S. Navy Air Development Squadron 6, flying Hercules C130 aircraft, placed the scientific party in the field and maintained it for 83 days. A U.S. Army aviation detachment using three UHIB turbine helicopters provided close air support for the field programs on the surface. We used a U.S. Navy LC117 aircraft for the aeromagnetic survey.

Camp Neptune (83°34′ S., 57°25′ W.) (pl. 1), the base station of operations for this project, was located about 2,200 km from the main U.S. Logistics Base in Antarctica at McMurdo Sound. The 34-man field party was composed of 18 scientists and topographic engineers, 1 United States–Antarctic Research Program representative, 1 Navy aerographer, and 14 officers and men of the Army Aviation Detachment; 6 additional Navy personnel were at the field camp during the aeromagnetic survey. The camp was in operation from October 26, 1965, until January 17, 1966.

We appreciate the assistance that we received during this investigation. Manfred Hochstein furnished unpublished data on the area west of the Pensacola Mountains. R. E. Wanous operated the magnetometer in the aeromagnetic surveys of 1963–64 and 1964–65. D. L. Schmidt and W. H. Nelson, geologists, and M. K. Weber, topographic engineer, assisted in making gravity observations at points visited in the course of their other work. E. R. Soza and the topographic control party made position and vertical angle elevation determinations. The U.S. Navy and U.S. Army provided logistic support. The National Science Foundation supported the research. C. R. Bentley of the University of Wisconsin Geophysical and Polar Research Center loaned the gravimeters, magnetometer, and seismic reflection equipment. L. Y. Bajwa assisted in computer processing. P. L. Williams, A. B. Ford, and D. L. Schmidt contributed through many helpful discussions.

GLACIAL AND BEDROCK PHYSIOGRAPHY

Ice-surface elevations in the area discussed in this report (fig. 2) range from about 100 m over the Ronne and Filchner Ice Shelves to more than 2,200 m south of the Patuxent Range. A major unnamed ice stream between the Patuxent Range and the Thiel Mountains drains a large part of the ice of East Antarctica into the Weddell Sea through the Ronne and Filchner Ice Shelves. Additional large amounts of ice enter the ice shelves through the Academy, Support Force, Slessor, and Recovery Glaciers (fig. 2; pl. 1).

A bedrock-elevation map (fig. 3) was compiled from seismic reflection measurements of ice thickness, or of ice and water thickness in ice-shelf-covered areas, supplemented by gravity measurements of ice thickness between seismic stations. This map is based on the results of the geophysical work described in a later section of this report and on the results of earlier oversnow traverses referred to previously. The highest elevations, as expected, are in the mountains, whose locations are indicated on plates 1 and 2. The approximate highest elevations are: Thiel Mountains, 2,800 m; Patuxent Range, 2,140 m; Neptune Range, 1,980 m; Forrestal Range, 2,070 m; Dufek Massif, 2,030 m; and Argentina Range, 920 m. The fact that the deepest seismic soundings are adjacent to the Dufek Massif, where the bedrock surface reaches depths of 1,730 m below sea level (pl. 1), indicates a vertical relief of about 4 km over a very short distance across the front of the Pensacola Mountains. This very high relief is probably due to faulting, as discussed in a later section.

A broad structural trough whose axis lies more than 1,500 m below sea level extends inland from the Weddell Sea to the Pensacola Mountains (fig. 3) (Behrendt, 1962a). This trough separates the main land mass from a shallow area (less than 300 m below sea level) that extends well into the Weddell Sea north of the ice front. This shallow area was called Berkner Bank by Behrendt (1962a), who suggested that the area is a large buried moraine. Deep channels

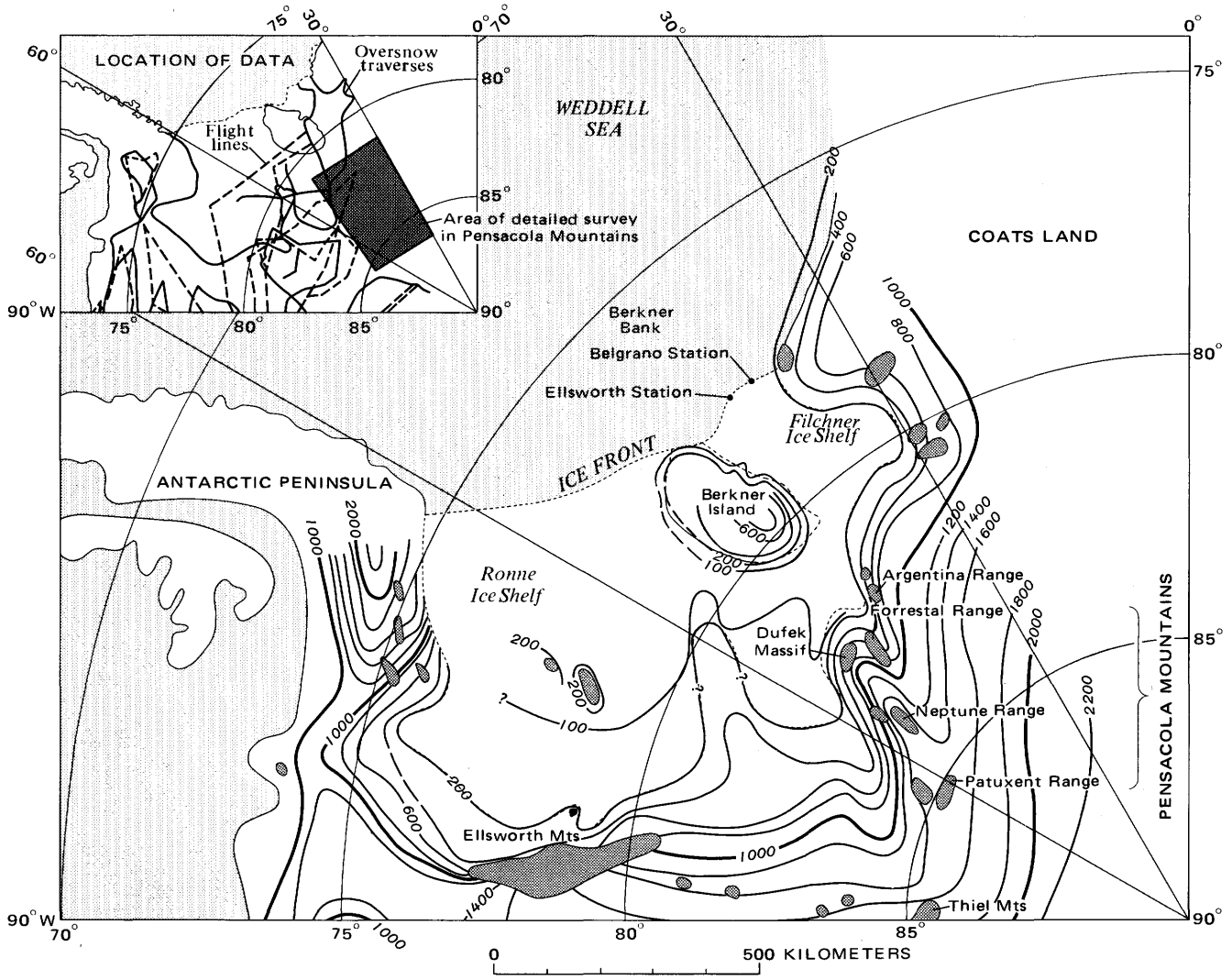

FIGURE 2. — Snow-surface-elevation map. Contour interval 200 m; 100-m contours shown on ice shelf. Exposed bedrock shown by heavy shading. Inset map shows location of oversnow traverses and flightlines used in compilation.

between the various ranges in the Pensacola Mountains (fig. 3) probably originated by glacial erosion, as suggested by geologic relations. In general the Pensacola Mountains appear to be a block elevated 2–3 km above the surrounding bedrock beneath the adjacent ice-covered areas. The bedrock surface between the Thiel and Pensacola Mountains reaches depths of about 1 km below sea level, and inasmuch as this bedrock depression is separated from the trough to the north, it is probably a tectonic, not an erosional, feature.

SUMMARY OF GEOLOGY

PRECAMBRIAN AND PALEOZOIC ROCKS

The geology of the Pensacola Mountains has been discussed by Schmidt and Ford (1969), Ford and Boyd (1968), Williams (1969), Schmidt, Dover, Ford, and Brown (1964), and Schmidt, Williams, Nelson, and Ege (1965). We quote and paraphrase extensively from these reports in this summary. Schmidt and Ford's (1969) geologic map was published at the same scale and on the same base as the plates in this report and should be used in conjunction with these plates. We have generalized their geology, as shown on plate 1, and have modified their geologic column, as shown in figure 4.

The Pensacola and Thiel Mountains are part of an ancient tectonic belt nearly coincident with the present Transantarctic Mountains. Rocks of the area consist of three sedimentary sequences bounded by major unconformities indicating at least three episodes of mountain building that took place during late Precambrian, early Paleozoic, and early Mesozoic time. The oldest rocks in the Pensacola Mountains, designated the first sequence, are the Precambrian Patuxent Formation, which composes more than half the exposed rocks. This formation is a thick succession (at least 10 km) of terrigenous sandstone and shale of turbidite origin, containing interbedded pillow lavas and basalt flows

in several areas. Volcanism occurred at various times during the deposition of Patuxent sediments; many diabase sills and a few felsic sills and plugs were injected into them.

In late Precambrian or Early Cambrian time, the Patuxent Formation was tightly folded and weakly metamorphosed. During subsequent marine transgression, Cambrian and Cambrian(?) limestone, felsic flows and pyroclastic rocks, siltstone and mudstone, and volcanic rocks were deposited, composing the Nelson Limestone, Gambacorta Formation, and Wiens Formation of the second sequence. At the end of Cambrian time, Cambrian and Precambrian rocks were folded and refolded respectively. The sedimentary rocks were intruded by rhyolite porphyry sills and, in the Washington Escarpment area, by a thick granitic pluton with a Rb-Sr age of 510 m.y. (million years) (Early Ordovician or Late Cambrian) (Schmidt and Ford, 1969).

After a period of erosion, a third sequence was deposited, consisting of the Neptune Group and Dover Sandstone of early(?) to middle Paleozoic age and the Gale Mudstone and Pecora Formation of late Paleozoic age. From base to top, the Neptune Group consists of the Brown Ridge Conglomerate, 0–1,000 m thick, the Elliott Sandstone, which is coarse grained and carbonate cemented, 700 m thick; the Elbow Formation, interbedded siltstone and fine-grained sandstone, 300 m thick; and the quartzose Heiser Sandstone, 300 m thick. Disconformably above the Neptune Group is the quartzose Dover Sandstone, 1,000 m thick, and the Gale Mudstone, a tillite, about 200 m of which is exposed. In the Pecora Escarpment and the southern Forrestal Range, well-bedded light-tan quartzose sandstone, siltstone, and shale have many conspicuous interbeds of carbonaceous and coaly sediments that locally contain abundant fossil leaves of the Permian Glossopterid

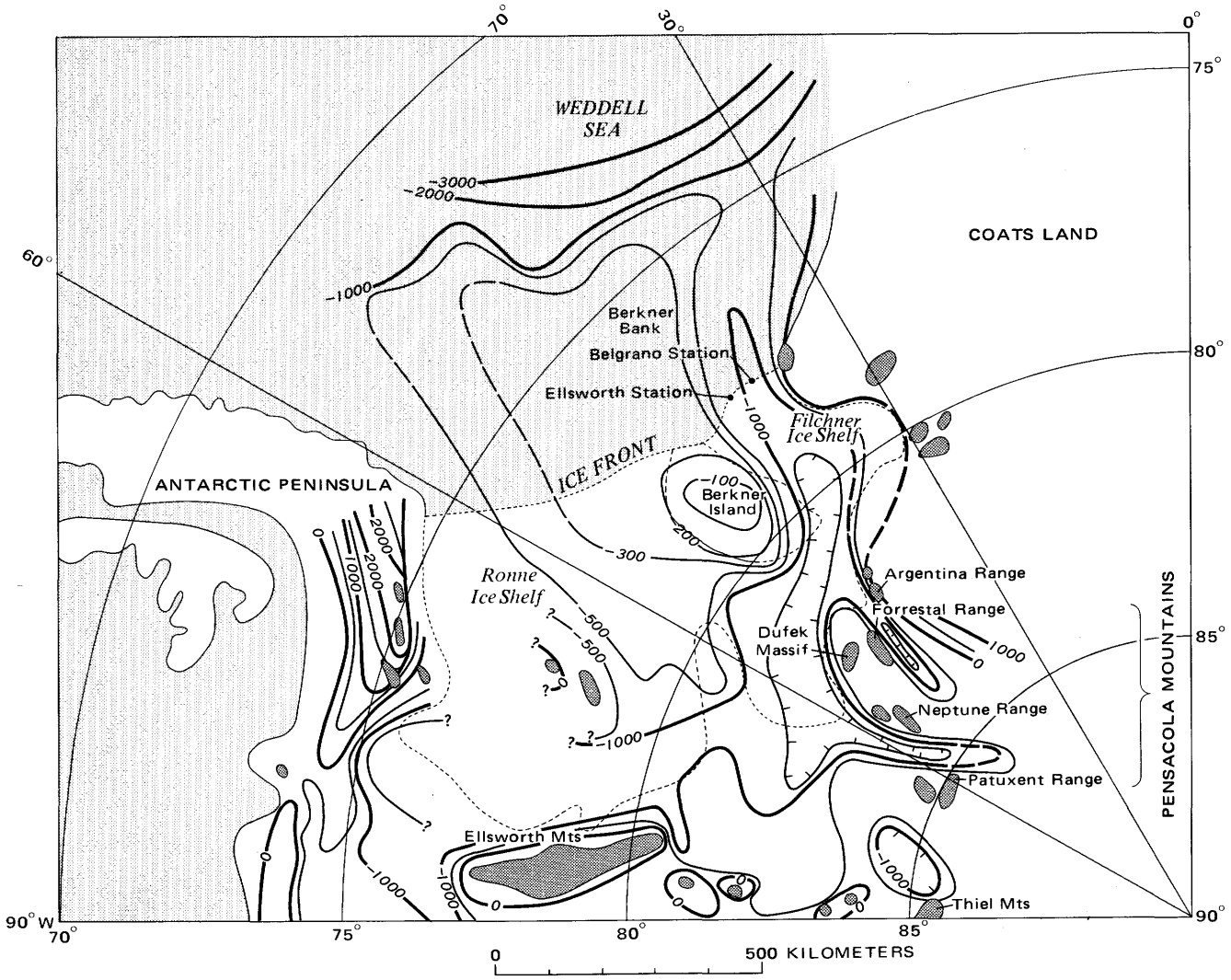

FIGURE 3. — Bedrock-elevation map. Seismic and gravity determinations on glacierized area; echo soundings on Weddell Sea. Contour interval 500 m; some 100-m contours shown in area of ice shelf. Exposed bedrock shown by heavy shading.

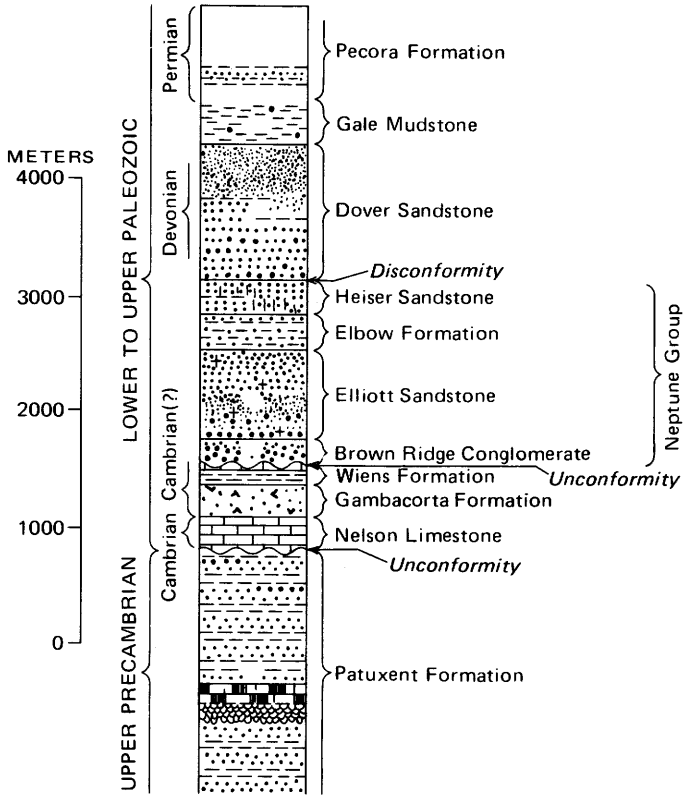

FIGURE 4. — Composite stratigraphic section for Pensacola Mountains. Modified from Schmidt and Ford (1969).

flora (Schmidt and Ford, 1969). These rocks are the Pecora Formation (Williams, 1969). The third sequence correlates with units generally termed "Beacon rocks" (formerly "Beacon Sandstone" and "Beacon Group") elsewhere in the Transantarctic Mountains.

After the Permian rocks were deposited, tectonic activity, probably Triassic in age (Ford, 1973), deformed the rocks of the third sequence into broad folds that are locally tight to overturned. In the Pecora Escarpment, the Pecora Formation was intruded by diabase in the form of thick sills. This diabase may be the equivalent of Ferrar Dolerite of probable Jurassic age commonly intrusive into Beacon rocks elsewhere in the Transantarctic Mountains.

DUFEK INTRUSION

Subsequent to the third tectonic episode, stratiform mafic rocks making up the Dufek Massif and most of the Forrestal Range were intruded. Ford and Boyd (1968) described the Dufek intrusion as predominantly pyroxene gabbro interlayered with minor anorthosite and pyroxenite and capped by granophyre. They indicated that 2 km of the upper part of the section, including the granophyre zone, is in the Forrestal Range and 2 km of a nonoverlapping lower part of the section is in the Dufek Massif. The layers in the intrusion dip gently southeastward, and in the Forrestal Range they form a broad deformed and faulted syncline. Ford (1973) cited an age of 168±5 m.y. (Middle Jurassic) for plagioclase from Dufek gabbros.

The general shape of the Dufek intrusion is not known, although we can infer something about the configuration from the magnetic data. Much of the intrusion lies buried by the thick ice sheet. The only exposure of a contact with country rock is in a small area in the southern Forrestal Range. There, Ford (1970) noted that the recrystallized Dover Sandstone is cut at a high angle by fine-grained gabbro adjacent to the upper strata of the main layered series. The floor of the intrusion is not exposed anywhere. Ford pointed out major dissimilarities between the Dufek intrusion and typical examples of both funnel-shaped and lopolithic intrusions. In the Dufek intrusion, the ratio of the horizontal to the vertical dimension is at least 20 : 1, which argues against a simple funnel shape for the body, whose walls would project to converge, if they ever did, at abyssal depths in the subcrust or mantle. The gravity data and magnetic data would not allow this. The great horizontal-to-vertical dimension ratio indicates a sheetlike form for the intrusion. Ford and Boyd (1968) illustrated a cross section showing a broad floor, but Ford (1970) pointed out that the term "lopolith" could not be used, because this would require a general concordancy. The contact of the Dufek intrusion is highly discordant to sedimentary country rock structures (geologic map of Schmidt and Ford, 1969) as well as to subhorizontal internal layering of the intrusion. Ford believed that the lopolithlike synclinal form of the layered intrusion has resulted from weak folding. There is no evidence of feeder location or structural control. The major folds in the country rock show little evidence of disturbance by intrusion. Inclusions of metamorphosed country rock are too few to suggest that stoping was a significant process.

Ford (1970) suggested two possible explanations for the absence of roof rocks: (1) they may have been removed by erosion accompanying hydraulic lifting of the roof during a "passive" emplacement of the magma, or (2) they may have never existed at all, assuming Daly's (1933) concept of the extrusive origin of an igneous complex as a composite lava flow. Ford cited several arguments against an extrusive origin, however, and concluded that the contact relationships are more in accord with intrusive than with extrusive emplacement. The absence of shock metamorphism phenomena appears to rule out an astrobleme origin.

Although the rocks of the Dufek intrusion are chemically and mineralogically varied, Ford believed, on the basis of smooth chemical trends for rocks throughout the layered mafic series and in the 300-m-thick granophyre cap, that they form a single comagnetic series. He noted that trends of most elements of the Dufek intrusion broadly parallel those of the Skaergaard intrusion in Greenland and of other highly differentiated layered mafic intrusive bodies, although conspicuous differences occur, probably due to differences in composition of parent magmas. The Dufek

rocks remain SiO_2 saturated throughout the entire stratigraphic section.

Figure 5, from Ford (1970), shows the mafic index as it varies with stratigraphic level in the Dufek intrusion. The data in this figure should be compared with the magnetic data over the Dufek intrusion discussed in the following sections.

There is a general increase upward in the section in iron oxide, magnetization (Beck and Griffin, 1971), and density (Ford and Boyd, 1968). The densities increase upward from about 2.8 to 3.1 g/cm³, an increase of about 11 percent. The magnetizations in the intrusion, as measured by Beck and Griffin (1971), show a range from less than 0.00001 emu/cm³ near the base of the section to 0.015 emu/cm³ near the top, a change of about three orders of magnitude. Their data show a high remanent magnetization component, with Q (ratio of remanent to induced magnetization) ranging from 1.3 to 5. The increase in magnetization with height in the intrusion (fig. 6) shows correlation coefficients for K_a (susceptibility) and for J_r (remanent magnetization) of 0.72 and 0.33 respectively (Beck and Griffin, 1971). These authors cited a correlation coefficient between K_a and J_r of 0.57. The much greater variation in magnetization compared with density is reflected in the magnetic and gravity maps discussed later in this report.

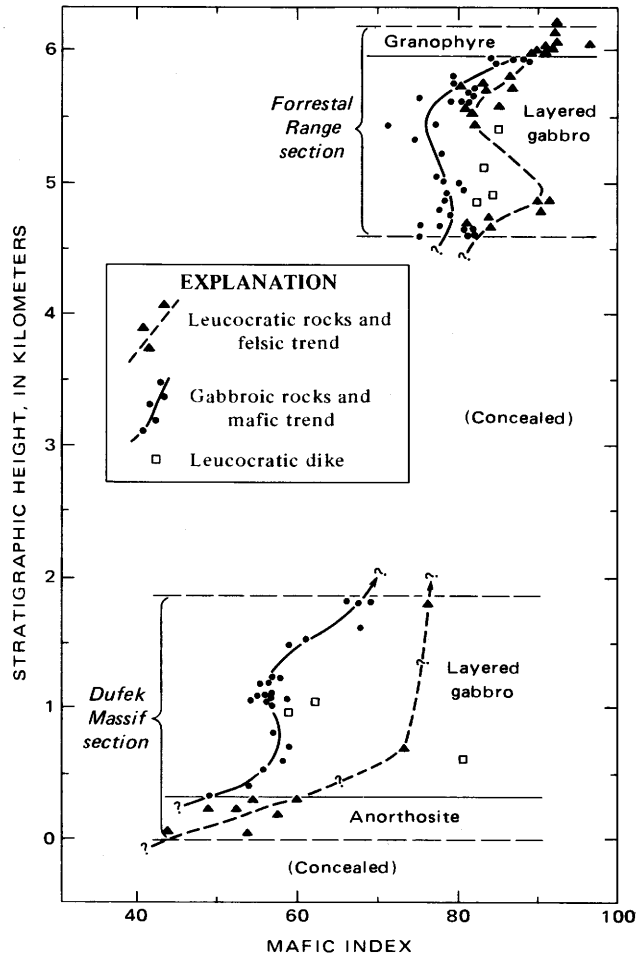

FIGURE 5. — Variation in mafic index, $\frac{FeO + Fe_2O_3 \times 100}{FeO + Fe_2O_3 \times MgO}$, with height in the Dufek intrusion. From Ford (1970).

LATEST TECTONIC ACTIVITY

Schmidt and Ford (1969) and Ford (1970) described final periods of tectonic activity including weak deformation in latest Mesozoic and Tertiary time, perhaps related to continental block movements on a large scale which caused broad flexing of the consolidated stratiform intrusive mass. They also cited probable late Cenozoic epeirogenic uplifts to account for high-angle faults that locally disrupt the Dufek gabbro along the northwest front of the Pensacola Mountains.

GEOPHYSICAL INVESTIGATIONS

GRAVITY SURVEY

We used one Worden and two LaCoste and Romberg geodetic gravimeters to make the gravity survey shown on plate 1. The Pensacola survey base station at Camp Neptune was tied four times, after periods of several hours each, to the McMurdo base station (Behrendt and others, 1962). An additional check on the Pensacola base station was made by reoccupying one of the 1957 IGY traverse stations on bedrock in the Dufek Massif (Behrendt, 1962b). This revealed a difference of +0.9 mgal, which is acceptable considering that the older data were all tied to North America by ship and oversnow vehicle (Behrendt and others, 1962) over a period of months and years. All gravity observations in this survey were tied to the Pensacola base station at Camp Neptune within a few hours, and errors in observed gravity are negligible.

Computer data from the gravity reduction program at Camp Neptune are shown in table 2, at the end of this report.

Absolute elevations are considered accurate within ±25 m (±5 mgal), and relative elevations, within ±10 m (±2 mgal). Two seismic reflections from the ice-water contact at the base of the Ronne Ice Shelf northwest of the Dufek Massif allowed a determination, by assuming hydrostatic equilibrium, of elevation. Corrections were made for changes in seismic velocity due to density increase in the upper ice shelf (Thiel and Behrendt, 1959), and absolute elevation accuracy at the reflection stations is conservatively estimated as ±10 m. The reflection stations were tied, one by vertical angle and one by altimetry, to the Pensacola Mountains control net. The elevations at stations in the survey were obtained from altimeter data corrected for temperature and for barometric pressure variations at a central control station. In addition, 97 gravity stations were on control points where vertical angle observations were made as part of the topographic mapping control. The standard deviation of the unadjusted altimetry data at the vertical

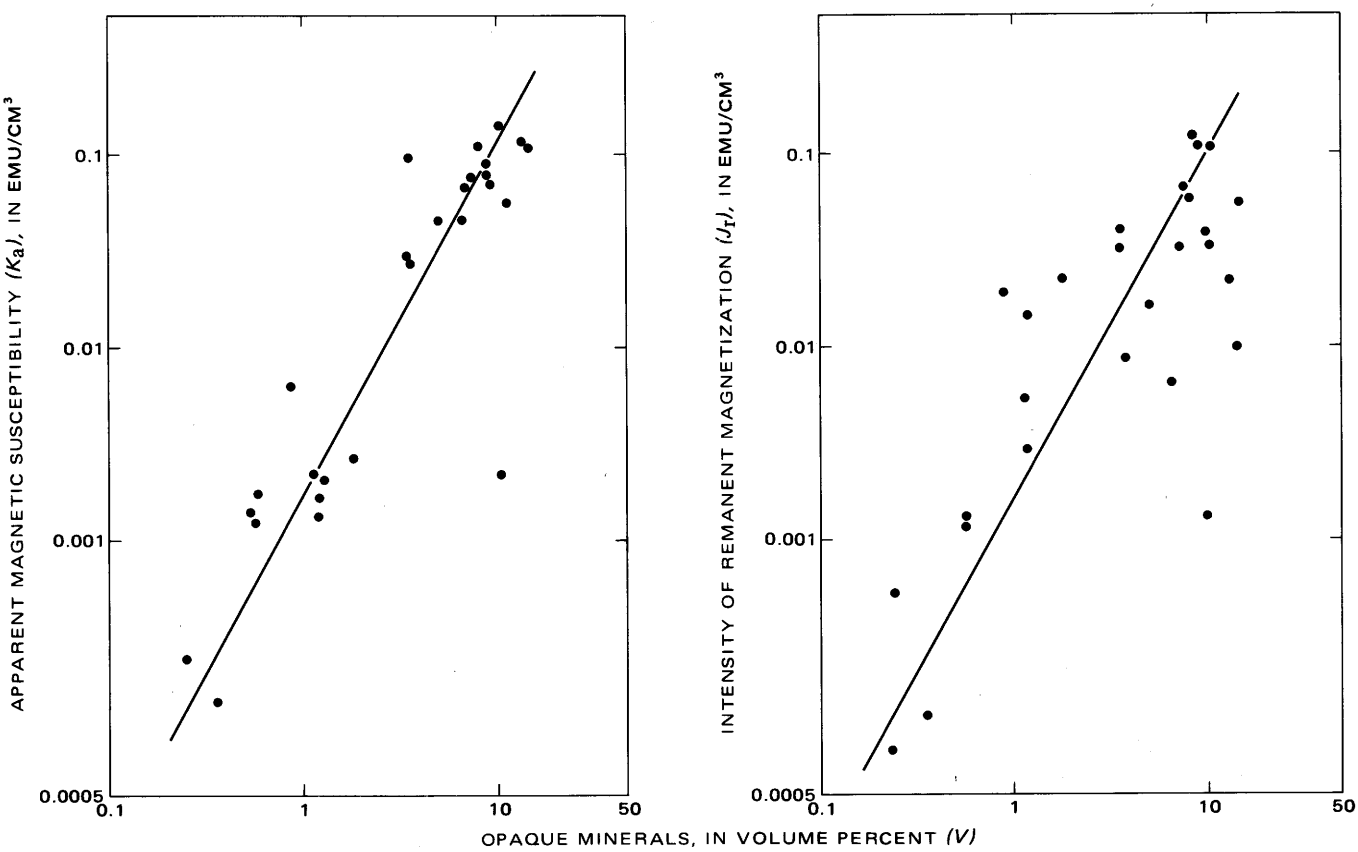

FIGURE 6. — Volume percentage of opaque minerals compared with apparent magnetic susceptibility and with intensity of remanent magnetization for samples from the Dufek intrusion. Lines are least-squares best fit. From Beck and Griffin (1971).

angle stations is ±12 m. All altimeter elevations were adjusted using the 97 vertical angle stations as control.

Positions of gravity stations at stations in the topographic control net are accurate to tenths of seconds, and stations away from the mountains, where graphical solutions of astronomical observations were made, are accurate to about a tenth of a minute. Therefore, latitude-correction errors are negligible.

Bouguer anomalies on the ice sheet are based on seismic reflection thickness measurements described in a later section. We made Bouguer corrections using densities of 0.9 and 2.67 g/cm^3 for ice and rock respectively. On grounded ice, the Bouguer correction was made in the usual manner by subtracting the effect, using appropriate densities, of slabs of ice and rock having a combined thickness equal to the elevation. If the ice-rock contact was below sea level, we made an additional correction by adding the effect of a slab having a density of 1.77 g/cm^3 (density of rock minus density of ice) and a thickness equal to the thickness of the ice below sea level. For seismic stations on floating ice the Bouguer correction was made assuming hydrostatic equilibrium of the ice shelf and correcting the free-air anomaly from sea level to bedrock by adding the effect of a slab having a density of 1.64 g/cm^3 (density of rock minus density of sea water) and a thickness equal to the depth of bedrock below sea level.

The largest source of error and the most difficult to evaluate is the terrain effect. Terrain corrections could not be made, as they usually are in other parts of the world, because of insufficient detail on the best available maps (1 : 250,000 scale, 200-m contour interval). In addition, a large unknown effect due to subglacial terrain could not be corrected for, even if larger scale maps had been available. The corrections could be as great as several tens of milligals at certain stations, but experience suggests that they should be 10 mgal or less for most stations. We attempted to allow for terrain effects in contouring the maps by assuming that all corrections for stations on rock would be positive and that the complete Bouguer anomaly (unknown) must be at least as positive as the simple Bouguer anomaly.

MAGNETIC SURVEY

Total magnetic intensity measurements were made along the lines indicated on the magnetic maps (pl. 2). We used an Elsec-Wisconsin proton precession magnetometer (Wold, 1964), flown in a LC117 aircraft at a constant barometric elevation of 2,100 m. Trimetrogon photography, available at the time of the survey, provided position control in the

area of the mountains. Dead reckoning and solar observations, adjusted to photo-identified points indicated, were the only control at the northwest and southeast ends of the lines over the featureless ice sheet. Consequently, position errors are variable but are minimal near the control points. Some lines crossed no identifiable rock outcrops, and these have greater position errors. A reliable quantitative error estimate is difficult to obtain, but at the ends of the lines the errors probably amount to several kilometers. Diurnal control was obtained from a baseline connecting the profiles.

Total magnetic intensity values of the Pensacola Mountains area are shown on the three maps of plate 2. Because of the widely spaced flightlines, position uncertainties, and relatively low amplitude and areal extent of the anomalies over most of the area, we decided that the profiles themselves would provide the most geologic information except in the area of the Dufek intrusion. Fortuitously the flightlines approximately parallel the main field contours, so we did not remove any regional gradient in the profiles shown on plates 2*A* and 2*B*. Plate 2*A* shows the "high gain" display of the magnetic profiles. High-amplitude anomalies over the Dufek intrusion have been omitted because at this scale the amplitudes are so great that they would not be adequately displayed. The line numbers refer to the preflight designations of the planned magnetic survey. In the actual flying of the survey, some lines were omitted. Plate 2*B* shows the high-amplitude magnetic anomalies over the area of the Dufek intrusion. The "gain" is lower by a factor of 5 compared with that used for plate 2*A*. Only the profiles over the high-amplitude anomalies are indicated. Plate 2*C* shows a residual total magnetic intensity map of the area of the Dufek intrusion. The residual values, shown by the contours, were computed by removing the main earth field as a smooth curve along each flightline profile shown on plate 2*B* and along several additional lines indicated on plate 2*A*. We believe that this rather crude method is justified for the data on this map because of the high-amplitude anomalies and large contour intervals. As in any contouring, some interpretation and inference were required.

SEISMIC REFLECTION MEASUREMENTS

Because radar depth sounding equipment was not available to us at the time this survey was made, we used the more traditional seismic reflection measurements for obtaining ice thickness values. These measurements were necessary for the Bouguer gravity reduction, as discussed previously, as well as for general topographic information. We used the Texas Instruments 7000B seismograph system with 12 geophones spaced 30.5 m apart. Charge size was usually 500 g of ammonium nitrate at shot depths of 4–8 m. UHIB helicopters were used to occupy the seismic stations.

Seismograms from two typical reflection stations are shown in figures 7 and 8. Figure 7 presents two seismograms from station 2 on the Ronne Ice Shelf. This shelf is one of the thickest in the world; the ice is 1,270 m thick, and the bedrock is 1,470 m below sea level. As mentioned in the preceding gravity section, we used the ice-thickness determination from this station and from station 3 to determine an absolute elevation for the Pensacola Mountains survey. Use of a velocity of sound in ice of 3,810 m/s and a mean density of the ice shelf of 0.894 g/cm^3 was based on results in the Filchner and Ross Ice Shelves during the IGY (Thiel and Behrendt, 1959; Thiel and Ostenso, 1961). We used the R_1 reflection to determine the thickness of the ice shelf as 1,266 m (this value was rounded off to 1,270 in table 1). Assuming hydrostatic equilibrium, we obtained a value of 167 m for the elevation at seismic station 2. Errors were conservatively estimated as follows: 50-m/s error in velocity would introduce a 2-m error in elevation, 0.01-sec error in reflection time would introduce a 2-m error in elevation, and 0.005-g/cm^3 error in mean density would introduce a 6-m error in elevation. Assuming all these errors to be in the

TABLE 1.—*Seismic reflection stations in Pensacola Mountains area, 1965–66*

[Question mark with figures indicates uncertain seismic reflection]

Seismic station (*, on ice shelf)	Gravity station	Lat	Long	Surface elevation (m ± 25 m)[1]	Reflection from base of ice (R_1) (sec)	Second reflection (R_2) (sec)	Water thickness (m ±20 m)	Ice thickness (m ±2½ percent)	Bedrock elevation (m)[2]	Free-air anomaly (mgal ±8 mgal)[4]	Bouguer anomaly (mgal ±12 mgal)[3]
*1	123	81° 51.4′	61° 19.8′	150	— — — —	[5]0.940	250	1,250	−1,350	−17	72
*2	122	82° 08.2′	59° 21.2′	167±10	[6]0.676	[5]1.178	360	1,270	−1,460	−34±3	66
*3	121	82°27′01″	57°16′09″	161±10	[4].653	[5]1.588	670	1,220	−1,730	−52±3	67
4	120	82°46′55″	54°52′03″	689	.300?			560?	130?	18	−18?
5	132	83°03′19″	51°52′27″	1,237	.225?			410?	830?	62	−46?
6	133	83°34.0′	45°04.1′	1,156	.710			1,340	−180	40	10
8	597	83°55.7′	38°58.5′	1,664	.37?			690?	970?	54	−80?
10a	74	83°29′38″	65°13′30″	513	.258			480	30	28	6
12	500	83°33′56″	57°24′41″	616	[6].750			700	−90	−15	−32
13	560	83°46′31″	54°07′58″	1,461	.346?			640?	820?	37	−79?
14	561	83°56′37″	50°32′09″	1,250	.838?			1,580?	−330?	−40	−63?
20	183	85°13.8′	82° 54.3′	1,431	1.288			2,440	−1,010	−50	−30
21	182	85°12.2′	78° 10.1′	1,378	1.220			2,310	−930	−46	−29
22	166	85°04.7′	71° 48.8′	1,344	.910			1,720	−380	3	−19
24	161	85°22.6′	60° 54.8′	1,524	.530?			990?	530?	57	−40?
25	162	85°35.7′	55° 47.2′	1,674	1.110			2,100	−430	8	−23
26	163	85°40.9′	53° 04.2′	1,723	[7]1.122	[5]1.175		2,130	−410	−4	−39
27	164	85°50.7′	48° 18.4′	1,845	1.385			2,600	−760	−41	−55

[1] Probable error except where indicated.
[2] Error is function of errors in surface elevation and ice thickness.
[3] Error is uncertain and variable; the ±12 mgal is estimated error due to combined errors in free-air anomaly and bedrock elevation. The unknown but possibly appreciable subice terrain errors would increase the true error.
[4] Ice-water reflection.
[5] Water-rock reflection.
[6] Probable multiple reflection.
[7] Ice-moraine reflection.
[8] Moraine-rock reflection.

same direction would give an error of ±10 m in the absolute elevation.

Several other interesting reflections are apparent in figure 7. R_1 is the first reflection off the base of the ice shelf; R_2 is the first reflection from the water-bedrock interface; R_3 is reflected off the water-rock interface, off the water-ice interface, again off the water-rock interface, and back to the surface; R_4 is reflected off the water-rock interface, back to the surface, off the ice-water interface, and back to the surface; and R_5 is the multiple reflection from the surface to the rock-water interface. Schematic travel paths for these reflections are indicated in figure 7.

Figure 8 shows a seismogram from station 26 in the southernmost part of the survey area. In addition to the first reflection, R_1, from the bottom, a second reflection, R_2, is apparent. We interpret R_1 as reflected off moraine because

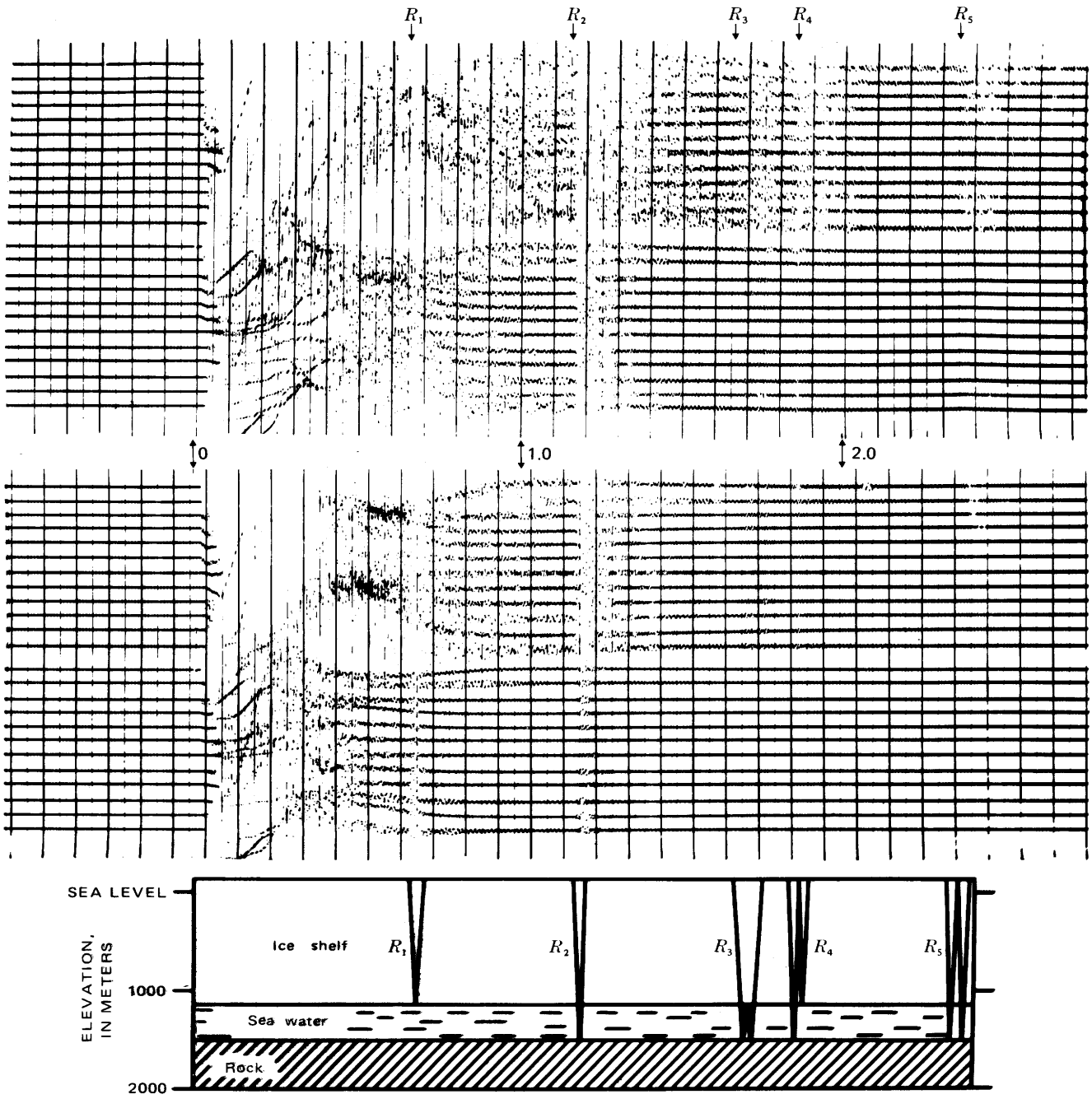

FIGURE 7. — Reflection seismograms for seismic station 2 (pl. 1). Reflections R_1 through R_5 correspond to travel paths indicated schematically below seismogram. Time, in seconds, is indicated between seismograms.

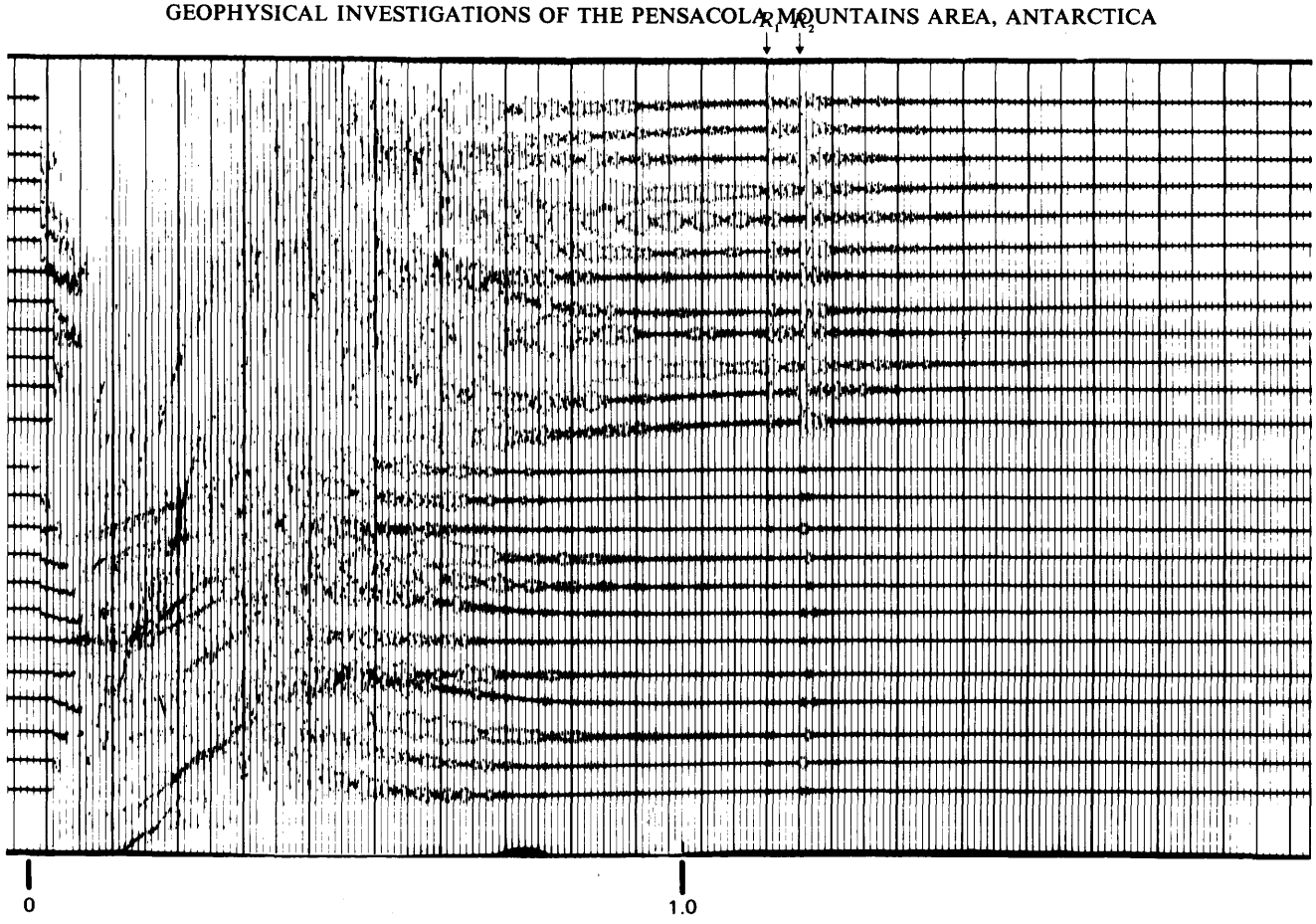

FIGURE 8. — Reflection seismogram for seismic station 26 (pl. 1). R_1 is reflection from base of ice at top of inferred morainal material. R_2 is reflection from inferred moraine-bedrock contact. Time, in seconds, is indicated at base of seismogram.

the amplitude is less than R_2, which we interpret as reflected off the solid bedrock. R_1 probably originates at the contact between the ice and the morainal material above the bedrock. Whether the material is frozen or not, which of course is unknown, would make a large difference in the seismic velocities. Assuming frozen moraine with a velocity of 4 km/s, the time difference between R_1 and R_2 would correspond to about 100 m of morainal material. If the moraine were not frozen, seismic velocity and the thickness might be only half this much. Either value would be reasonable.

Table 1 presents the principal facts for the seismic stations at which reflections were obtained. At some stations, the reflections were uncertain. Thicknesses were calculated using the relation:

$$H = ([t/2]-0.057)V_p+200,$$

where

H = ice thickness, in meters,
t = reflection time, in seconds, and
V_p = compressional wave velocity in ice, in meters per second.

The assumed V_p for grounded ice was 3,820 m/s (Bentley, 1964), for floating ice was 3,810 m/s (Thiel and Behrendt, 1959), and for sea water was 1,445 m/s (Thiel and Behrendt, 1959).

Free-air anomalies and bedrock-elevation differences measured at seismic reflection stations were used to compute bedrock elevations at stations on the ice sheet between the seismic reflection stations, using a constant of 20 m/mgal (Bentley, 1964). The resulting values were corrected for closure differences at the seismic stations; profiles of the bedrock relief along the seismic lines are shown in figure 9. These data plus others in surrounding areas from Behrendt (1961) and Manfred Hochstein (written commun., 1965) allowed us to construct the bedrock-elevation map of figure 3.

GEOPHYSICAL RESULTS

GRAVITY

NEPTUNE AND PATUXENT RANGES

Plate 1 shows the Bouguer anomaly map of the area of the survey, as well as the surrounding ice-covered area where data were available; figure 10 shows the free-air

anomalies. The most apparent feature of plate 1 is the broad gradient decreasing from northwest to southeast across the Pensacola Mountains. Values range from 82 mgal on the Ronne Ice Shelf northwest of Dufek Massif to −90 mgal in the northern Neptune Range. Scattered data to the east of the Pensacola Mountains at seismic reflection stations suggest that the Bouguer anomaly values increase somewhat in this area. Behrendt, Meister, and Henderson (1966) discussed this regional anomaly and suggested that it was a result of crustal thickening across the transition from West to East Antarctica. In the present report we discuss this interpretation and present some computed models. Superimposed on the broad regional anomaly are several shorter wavelength anomalies of several tens of milligals, which are of greater amplitude than the errors due to the topography and which have sources in the upper crust.

The steep linear gradient separating the Schmidt Hills from the Neptune Range lies along a fault mapped by D. L. Schmidt (unpub. data, 1973). The Schmidt Hills contain Precambrian diabase sills and probably have been uplifted from deeper within the crust. Whether the density contrast across the fault is sufficient to contribute to the steepness of the regional gradient is uncertain. The crustal models (fig. 11) computed along a profile in the vicinity of the Patuxent Range indicate a gradient as steep as that between the Schmidt Hills and the Neptune Range. Although diabase has not been mapped in the Rambo Nunataks area, which is crossed by this profile, it may well be present under the ice, and the gravity data indicate that the fault may continue this far south. The fact that magnetic data (pl. 2*A*) show anomalies in the area of Rambo Nunataks is consistent with the suggestion of diabase.

The high peaks of the southern Neptune Range, which have outcropping Cambrian sedimentary and igneous (volcanics and sills) rocks, have an associated positive anomaly of 10−20 mgal relative to the Patuxent Formation in the northern Neptune Range and about 20−30 mgal relative to the middle and upper Paleozoic rocks mapped on the flanks. A negative anomaly occurs on the west side of the southern Neptune Range over the middle and upper Paleozoic rocks. These gravity differences are suggestive of the relative variation in thickness of the upper and middle Paleozoic, Cambrian, and Precambrian sedimentary rock units. Because a greater contrast is unlikely, a density contrast of 0.1−0.2 g/cm³ between different Paleozoic or Precambrian sedimentary rocks was used to estimate relative thickness variation; a 10- to 30-mgal difference in gravity corresponds to a 2.4- to 7.2-km difference in thickness for a density contrast of 0.1 g/cm³ and to half as much for a contrast of 0.2 g/cm³.

A negative anomaly of at least −30-mgal amplitude occurs over the granite of Median Snowfield and the middle and upper Paleozoic sedimentary rocks in the Washington Escarpment area, relative to the Patuxent Formation in the Neptune Range. The granite must be of lower density than the Patuxent Formation if it is the source of this anomaly. Because densities for granite possibly could be as low as 2.5 g/cm³ (Woollard, 1962), the granite of Median Snowfield is assumed to be the anomaly source. It is not easy to separate the effect of the middle and upper Paleozoic rocks from the effect of the underlying granite in the Washington Escarpment area because of a probable low density contrast between these rock units. The combined thickness of granite and sedimentary rocks could be as great as 7.2 km if the density contrast relative to the Patuxent Formation is 0.1 g/cm³.

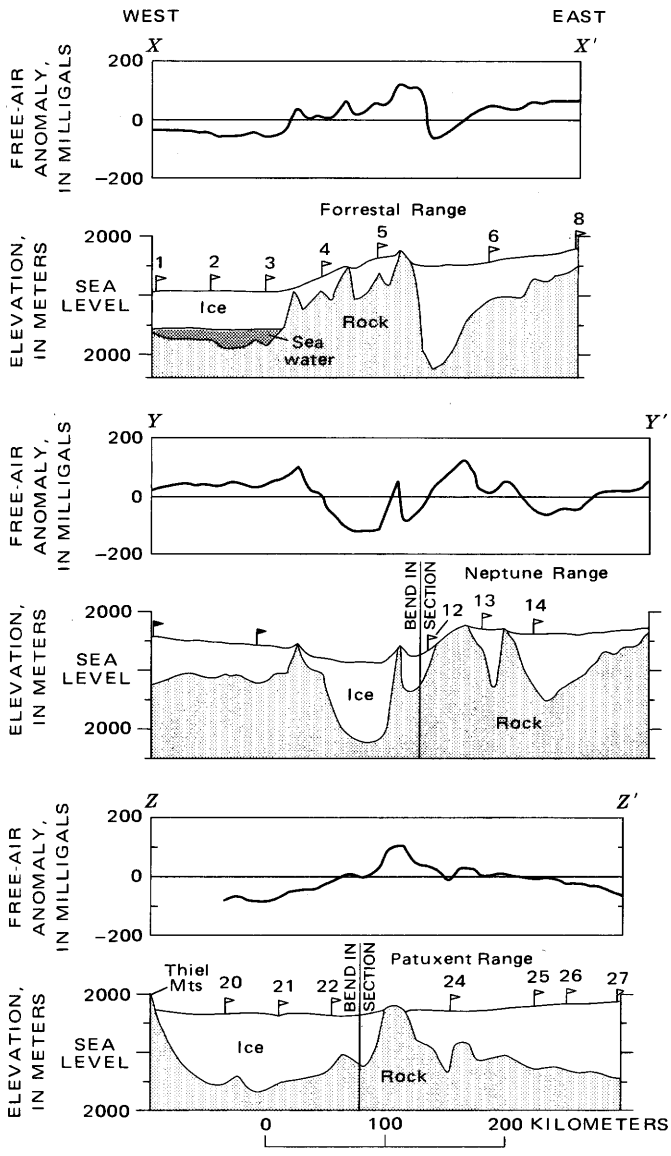

FIGURE 9. — Surface- and bedrock-elevation and free-air gravity-anomaly profiles along seismic traverse lines $X-X'$, $Y-Y'$, and $Z-Z'$ (pl. 1). White flags indicate seismic reflection stations; black flags, Manfred Hochstein's reflection stations. Bend in sections $Y-Y'$ and $Z-Z'$ approximately located.

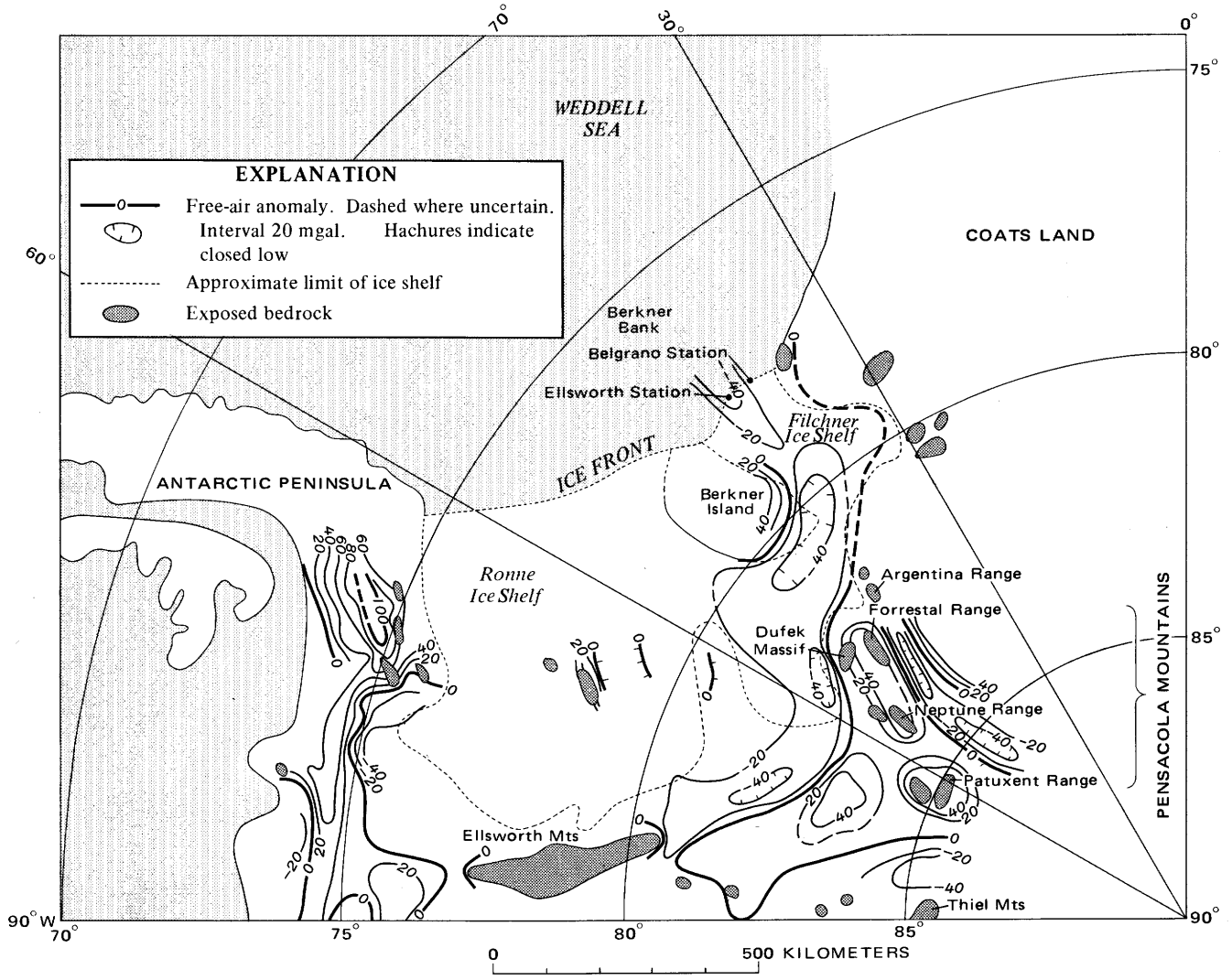

FIGURE 10. — Free-air-anomaly map. Data observed along traverses shown on index map in figure 2.

The gravity field in the Patuxent Range area, other than the regional gradient mentioned previously, is relatively smooth. A positive gravity anomaly with a 20-mgal closure in the northern part of the range, over the Patuxent Formation, apparently extends over the Academy Glacier and may be significant, but we are not yet able to evaluate it precisely. A negative magnetic anomaly (pl. 2*A*) over the same area as this positive gravity anomaly suggests a mafic intrusion with reversed magnetization. Other closures within broader contours in the Patuxent Range and Pecora Escarpment area have amplitudes that are probably too close to the noise level of the data to be significant.

DUFEK INTRUSION

Bouguer anomaly contours over the mapped extent of the Dufek intrusion range from 40 mgal in the northwest to −60 mgal in the southeast. The total range in the Pensacola Mountains area is from 82 to −90 mgal across the transition from West to East Antarctica. The mass effect of the Dufek intrusion distorts the regional gradient, as is apparent on plate 1. The amplitudes of the anomalies due to the effect of the Dufek gabbro are much larger than the errors due to the effect of the terrain.

Correlation of the gravity contours with the Forrestal Range and Dufek Massif areas is apparent. Unfortunately, because the anomalies associated with these ranges are superposed on the regional gradient, it is not practical, considering the general sparsity of data, to separate the effect of the Dufek intrusion from the regional change due to lower crustal structure.

In an attempt to estimate the amplitude of the anomaly associated with the Dufek intrusion we plotted all the gravity data in the Pensacola Mountains area against elevation (fig. 12). The regression line was calculated using weighted means for elevation intervals of 200 m and Bouguer anomaly intervals of 10 mgal neglecting the

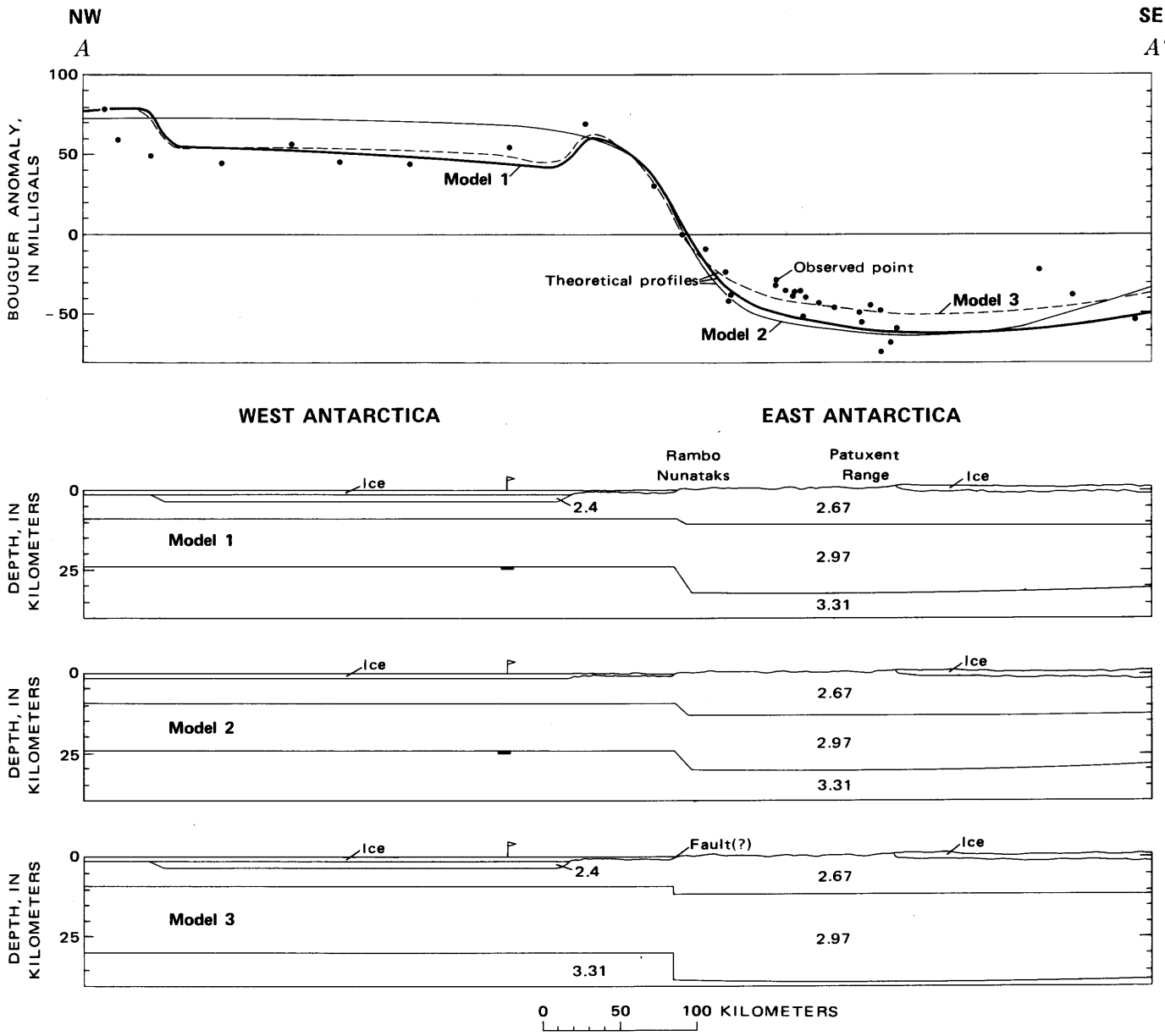

FIGURE 11. — Bouguer anomaly profile and theoretical crustal models along line $A-A'$ (pl. 1). The mass effect of ice has been included in the Bouguer reduction. Densities in models are indicated in grams per cubic centimeter. Flag indicates location of deep seismic reflection station; bar in models 1 and 2, the reflection itself.

stations on the Dufek gabbro. The maximum anomaly amplitude associated with the Dufek intrusion was estimated from the gravity difference between the regression line and the line of the same slope enclosing the data points on the positive gravity side of the graph (fig. 12). The gravity difference indicated is about 85 mgal — a reasonable estimate of the maximum gravity effect of the intrusion. A. B. Ford (written commun., 1972), using his measured densities, estimated a mean density for the intrusion of 2.98 g/cm³. If we assume a reasonable range of density contrast of 0.27–0.33 g/cm³, 85 mgal corresponds to about 8.8–6.2 km total thickness of the intrusion. This range is reasonable but is very uncertain because of the unknown density variation in the lower buried part of the intrusion.

We estimated the thickness of the Dufek intrusion at its south end, where we expected it to be thinnest. Comparison of the gravity contours in the southern Dufek Massif with those in the Cordiner Peaks to the southwest (over sedimentary rocks) suggests a difference of 20–40 mgal by projecting the regional trend northeast from the Cordiner Peaks. For a density contrast of 0.27 g/cm³, 20 mgal corresponds to 1.8 km thickness, and 40 mgal, to 3.5 km thickness. In other words, the base of the intrusion is probably 1.2–2.9

km below sea level where the base of the exposed section is at an elevation of about 600 m; unexposed thickness of the intrusion is therefore 1.8–3.5 km.

One of the main objectives in making the Pensacola Mountains geophysical surveys was to determine the lateral extent of the Dufek intrusion beneath the ice sheet, so we examined the gravity and magnetic data with this in mind. The 80-mgal closed contour northwest of the Dufek Massif occurs in an area of magnetic anomalies, described in the following discussion, which we interpret as being associated with Dufek gabbro. On the basis of the regional gravity we would expect a much lower value than the +10 mgal at the seismic reflection station near 83°30′ S., 45° W. We interpret this anomaly of several tens of milligals to be caused by a buried extension of the Dufek intrusion. This interpretation is supported by the magnetic data and is discussed later in this report.

CRUSTAL STRUCTURE

We have attempted to fit the Bouguer anomaly data observed on profile $A-A'$ (fig. 11; pl. 1), which extends across the boundary from West to East Antarctica in the vicinity of the Patuxent Range, to three idealized density models of the crust. Manfred Hochstein (Bentley, 1973) measured a reflection interpreted as coming from the crust-mantle interface at about 83° S., 70° W. He reported an average P-wave velocity, corrected for the ice, of 6 km/s in the crust and a depth to the M discontinuity of 24 km below sea level. Models 1 and 2 (fig. 11) are tied to this seismic sounding as indicated. The ice thickness is shown schematically but has not been included in the computed models because the Bouguer correction effectively adjusted the ice to a density of 2.67 (density used in the models). The main difference between models 1 and 2 is the inclusion of a 2.4-g/cm³-layer corresponding to low-density sedimentary

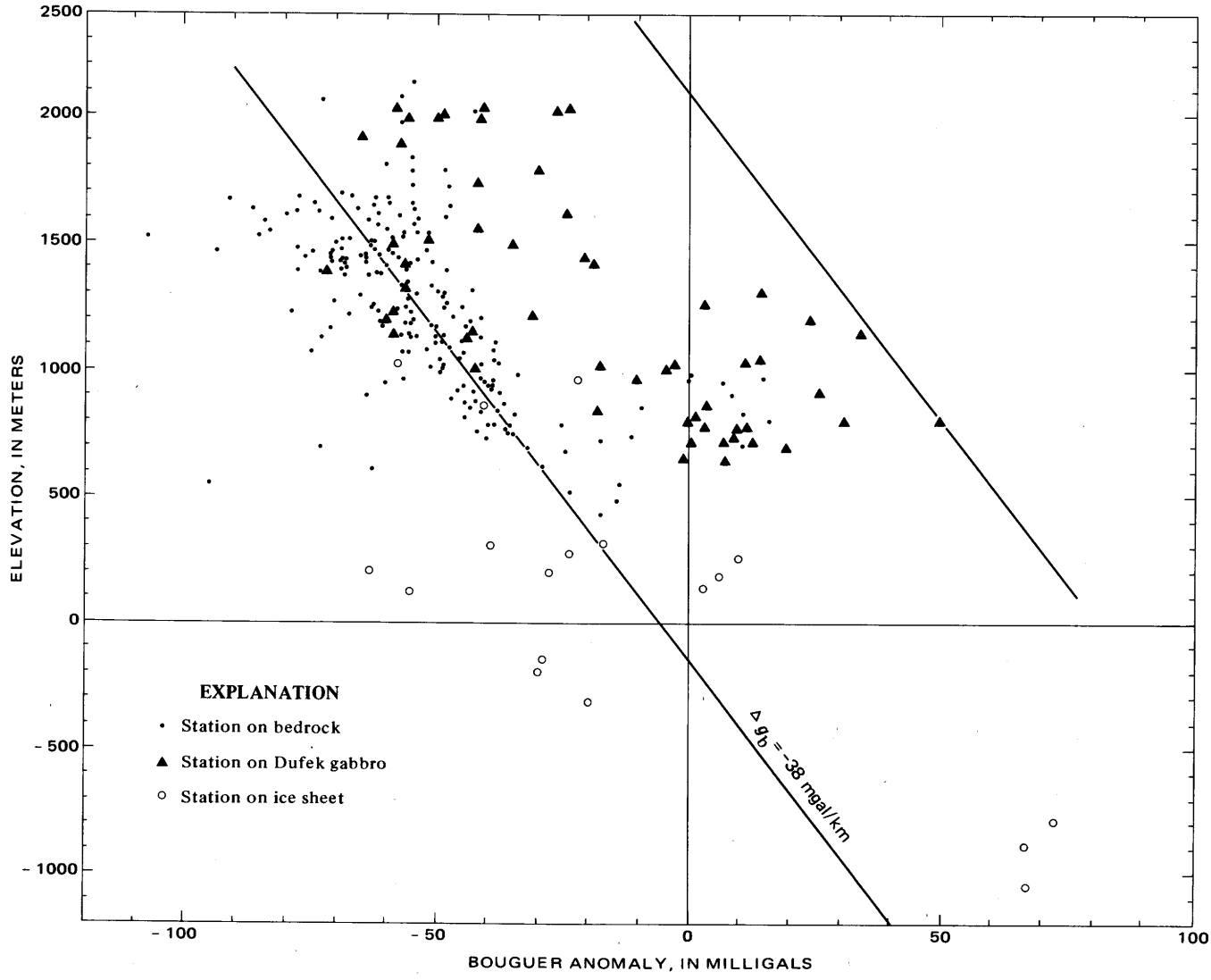

FIGURE 12. — Bouguer anomalies compared with elevation in the Pensacola Mountains area. The least-squares regression line was calculated from weighted means of elevation and Bouguer anomaly (Δg_b) for 200-m by 10-mgal areas of graph. The standard deviation is ±26 mgal, and the correlation coefficient is −0.72, which is significant at the 1-percent level.

rocks beneath the ice-covered area northwest of the mountains. As can be seen in this part of the section, the model 1 profile fits the observed data better than does the model 2 profile. Magnetic profiles suggest the existence of a significantly thick section of nonmagnetic, presumably sedimentary rock in this area (fig. 13). Although the density and thickness of any sedimentary rock in this area are highly speculative, the models appear to be reasonable approximations of the crust.

Model 3 (fig. 11) was computed ignoring the reflection sounding to mantle and assuming a value for continental margin crustal thickness of 30 km (depth to the M discontinuity) on the northwest side of the profile, as has been suggested by Robinson (1964) and Bentley (1964). A significant feature of model 3 is the vertical step at the crust-mantle interface required to fit the observed steep gradient. This step-like effect suggests a steeply dipping fault separating East and West Antarctica and has been postulated previously by Behrendt, Meister, and Henderson (1966) and Robinson (1964). Plate 1 indicates that the steep gravity gradient fitted by the models calculated for line $A-A'$ extends northeast; that gradient is coincident with a mapped fault separating the Schmidt Hills from the Neptune Range, as discussed in an earlier section. Model 3 would be consistent with the interpretation of deeper rocks upfaulted on the northwest side of the profile and would be compatible with the known geology (D. L. Schmidt, unpub. data, 1973). Of course, such a fault is also compatible with models 1 and 2.

To summarize the results of the crustal structural models of figure 11, we conclude either that the crust in the Pensacola Mountains area is abnormally thin on the West Antarctica side of the area, west of the front of the Pensacola Mountains, or that the crust has a normal thickness on the West Antarctica side with a steep faultlike step at the crust-mantle interface which may project to the surface in the area between the Schmidt Hills and the Neptune Range. Various writers (for example Craddock, 1970b) have presented continental reconstructions including Antarctica. (See fig. 18). One might expect a steep discontinuity at the crust-mantle interface if this steep gravity gradient marks the edge of the continent at the time of separation from Gondwanaland.

ISOSTASY

The free-air-anomaly map (fig. 10) and the free-air-anomaly profiles (fig. 9) show a high degree of correlation with bedrock topography (compare fig. 3), but the free-air anomalies in general average around zero. From both of these observations we can infer that the area is in approximate regional isostatic equilibrium. The Bouguer anomaly–elevation regression line in figure 12 has a zero elevation intercept of essentially zero Bouguer anomaly, within the scatter of the data, again suggesting regional isostatic compensation for the area of the survey. We do not consider the high free-air anomaly over the ranges in the Pensacola Mountains to be indicative of an isostatic anomaly, because we expect positive values of free-air anomaly over mountainous areas. For example, the southern Antarctic Peninsula area has a high average free-air anomaly (Behrendt, 1964), and yet computed models that assume regional isostatic compensation fit the observed data.

MAGNETIC RESULTS

DUFEK INTRUSION

Plate 2 shows the magnetic data of the Pensacola Mountains airborne survey. We have presented these data in three separate maps. Plate 2*B* shows the high-amplitude-anomaly profiles over the Dufek intrusion. Anomalies in this area, which approach 2,000 gammas amplitude from peak to trough (for example, profile 26), are highest over the Forrestal Range and decrease in amplitude from north to south over the Dufek Massif. Plate 2*C* shows contours of the anomalies in this area. As discussed in the section on geology, the work by Ford (1970) and the magnetic properties measured by Beck and Griffin (1971) indicate that the iron content, susceptibility, and remanent magnetization are greatest in the upper part of the intrusion in the Forrestal Range; they decrease downward through the section and are least in the lowest part of the intrusion in the southern Dufek Massif area (figs. 5 and 6). This gradation is consistent with the magnetic anomalies. Beck and Griffin (1971) reported high values of normal and reversed remanent magnetization. The effects of this high magnetization can be seen in the profiles of plate 2*B*, particularly on lines 21, 31, and 36. Because the uplift and erosion of parts of the intrusion have, in effect, stripped off various layers, we can magnetically examine successively lower parts of the section without the interference of high-amplitude anomalies in the upper part.

Figure 14 shows the magnetic profile along line 11 (pl. 2*C*). This figure compares the observed profile and the computed theoretical profile resulting from the model indicated. The topography is based on gravity and seismic data shown on plate 1. The very high magnetizations used in the model are typical of those measured in the upper part of the section of the Dufek intrusion and suggest mostly remanent magnetization in the rocks. This model does not purport to imply anything about the lower parts of the section. The theoretical profile supports the interpretation of a downfaulted part of the Dufek intrusion beneath the ice northwest of the Dufek Massif. On this basis, we conclude that the high-amplitude anomalies observed over the Ronne Ice Shelf on lines 6 and 11 and the lower amplitude anomalies along line 1 (pl. 2*B*) are caused by an extension of the Dufek intrusion.

Figure 15 shows observed and computed magnetic profiles along line 18 (pl. 2*C*). This profile is computed over a lower amplitude section of the intrusion, and magnetizations about an order of magnitude less than those

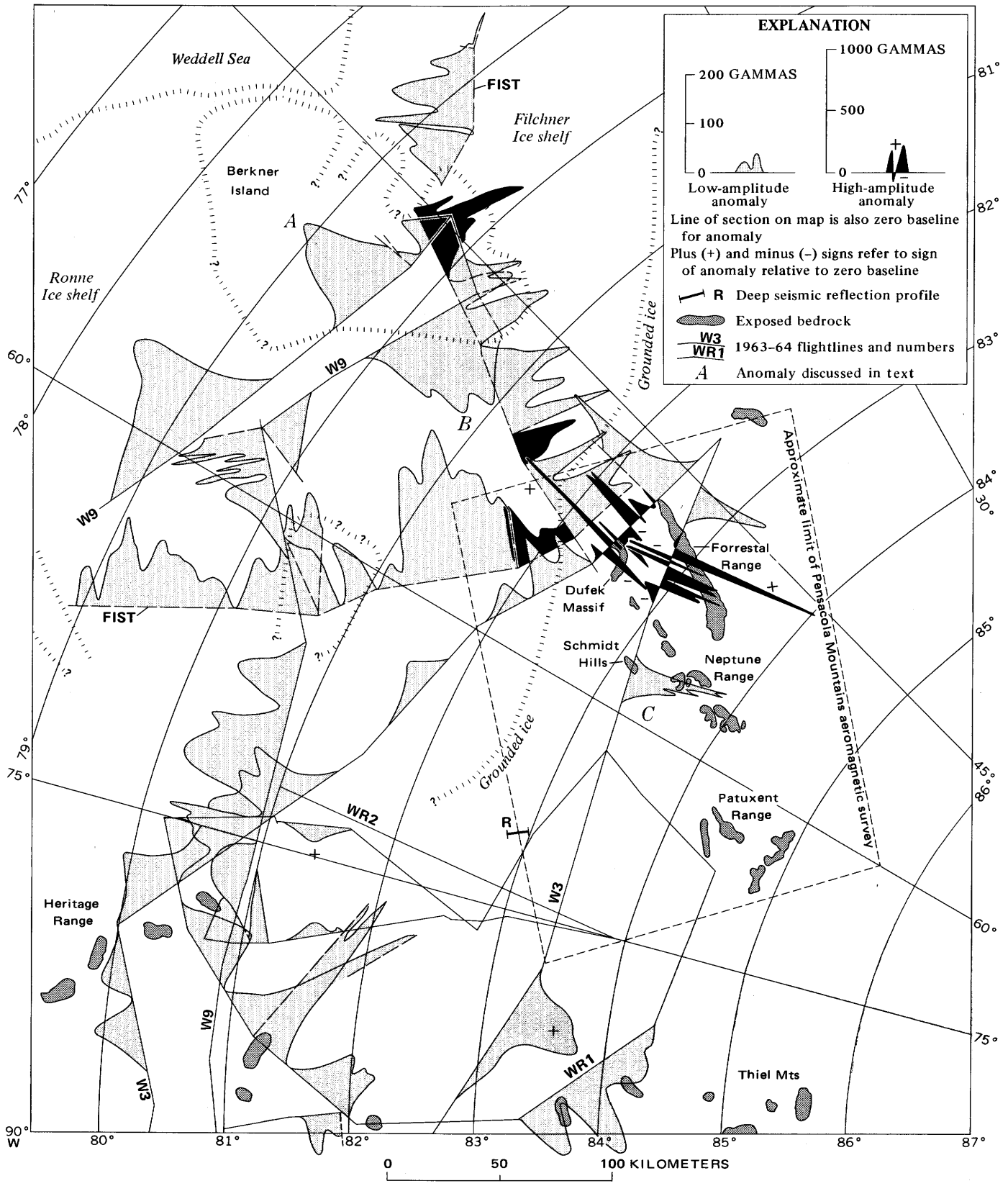

FIGURE 13. — Map showing magnetic anomalies along profiles observed prior to the collection of data shown on plate 2. Elevations of flightlines are variable but are generally about 1 km above snow surface. The only negative anomalies are plotted at the high-amplitude scale in the Dufek Massif and Forrestal Range area. FIST, Filchner Ice Shelf Traverse, 1957.

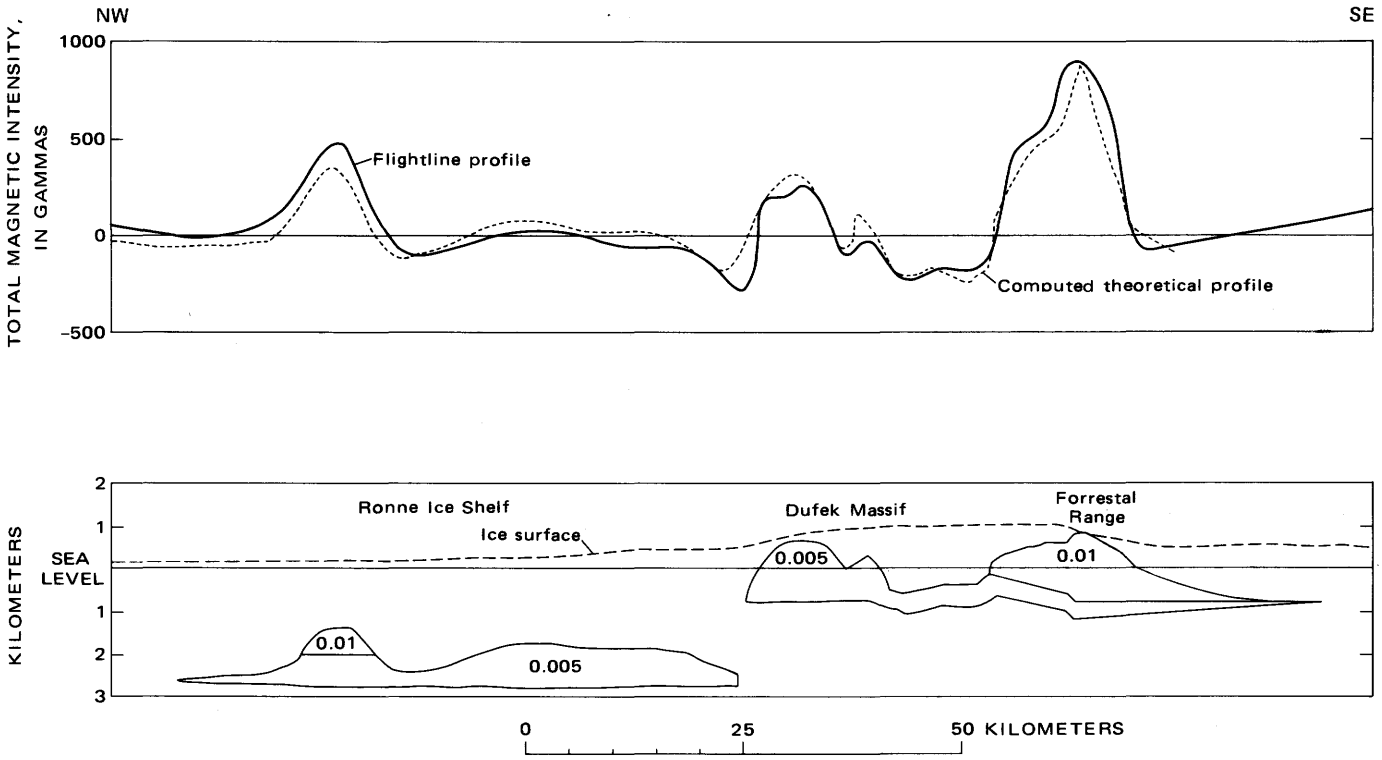

FIGURE 14. — Magnetic profile along line 11 (pl. 2C). Theoretical profile was computed for indicated model. Magnetizations are indicated in emu/cm³; all inclinations of magnetization are 70°.

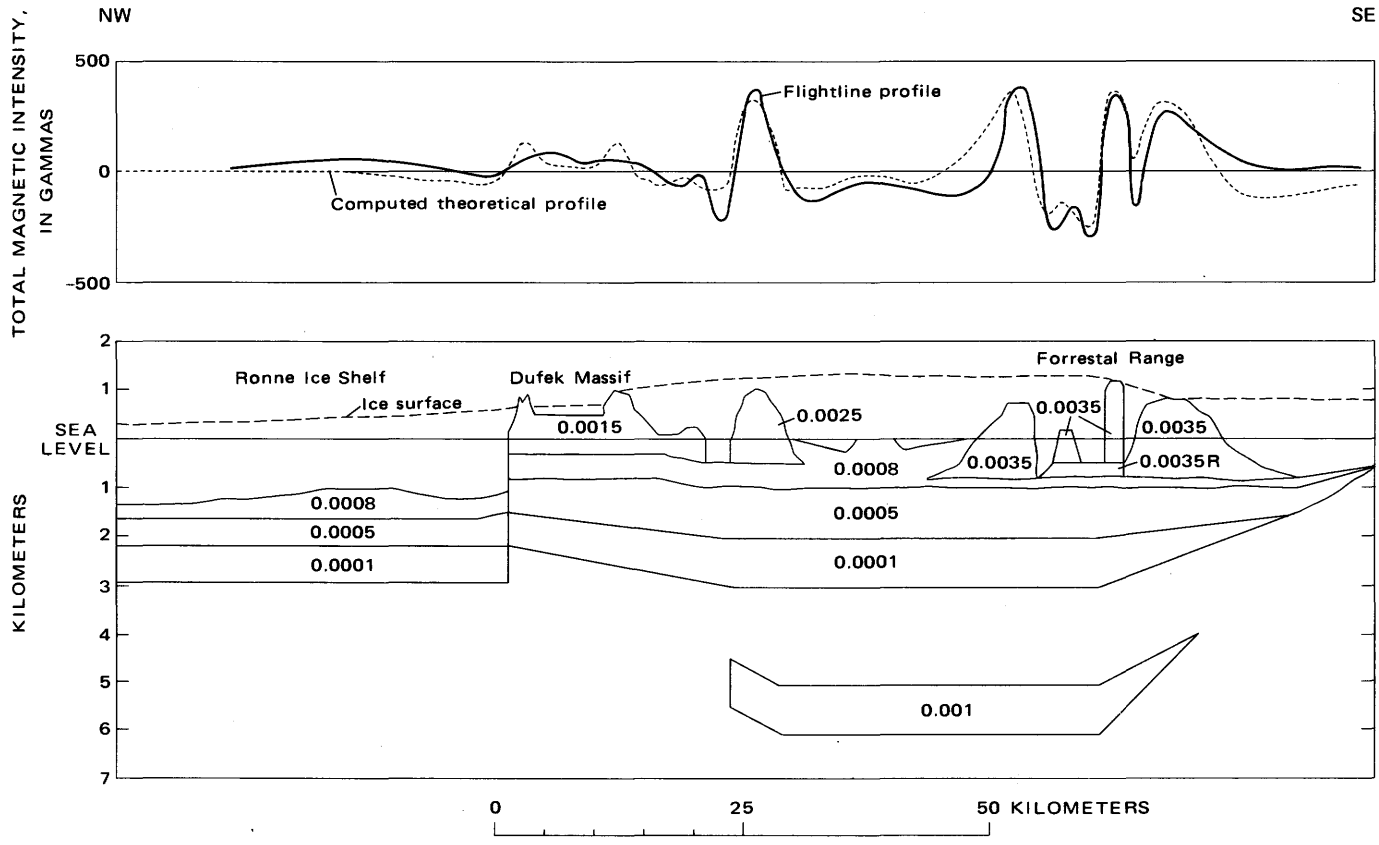

FIGURE 15. — Magnetic profile along line 18 (pl. 2C). Theoretical profile was computed for indicated model. Magnetizations are indicated in emu/cm³; all inclinations of magnetization are 70°; R refers to body having reversed magnetization.

of the model of profile 11 (fig. 14) are required to fit the observed data. A body with reversed magnetization was introduced to fit the data in the eastern part of the profile along line 18, as was the body at depth with the 0.001-emu/cm³ magnetization. The possible significance of a more magnetic layer at the base of the intrusion is discussed later in the report. Profiles in figures 14 and 15 show that the interpretation of continuity of the Dufek intrusion between the Forrestal Range and the Dufek Massif is consistent with the magnetic data.

Magnetic profile 26 (fig. 16) crosses the south end of the Dufek Massif (pl. 2*C*). Note that the vertical scale on this profile is greatly magnified compared with the scale in figures 14 and 15 because the amplitudes of the anomalies in this area are very much lower than those to the north. Theoretical profiles for two different models are fitted to the data from line 26 in figure 16. Very low magnetizations are required to fit these anomalies and are consistent with values reported by Beck and Griffin (1971) from rock samples collected in the area crossed by line 26. The depth to the base of the Dufek intrusion beneath the exposed section at the south end of the Dufek Massif, as suggested by model 1, is possibly about 2.5 km below sea level, but higher magnetizations than those measured in rock samples from this part of the section are required to fit the observed data. Model 2 provides a good fit to the observed data by using appropriately low magnetizations, but it requires infinitely thick bodies in the computed model and is therefore geologically unreasonable. These models imply either that a continuous low-magnetization section extends to great

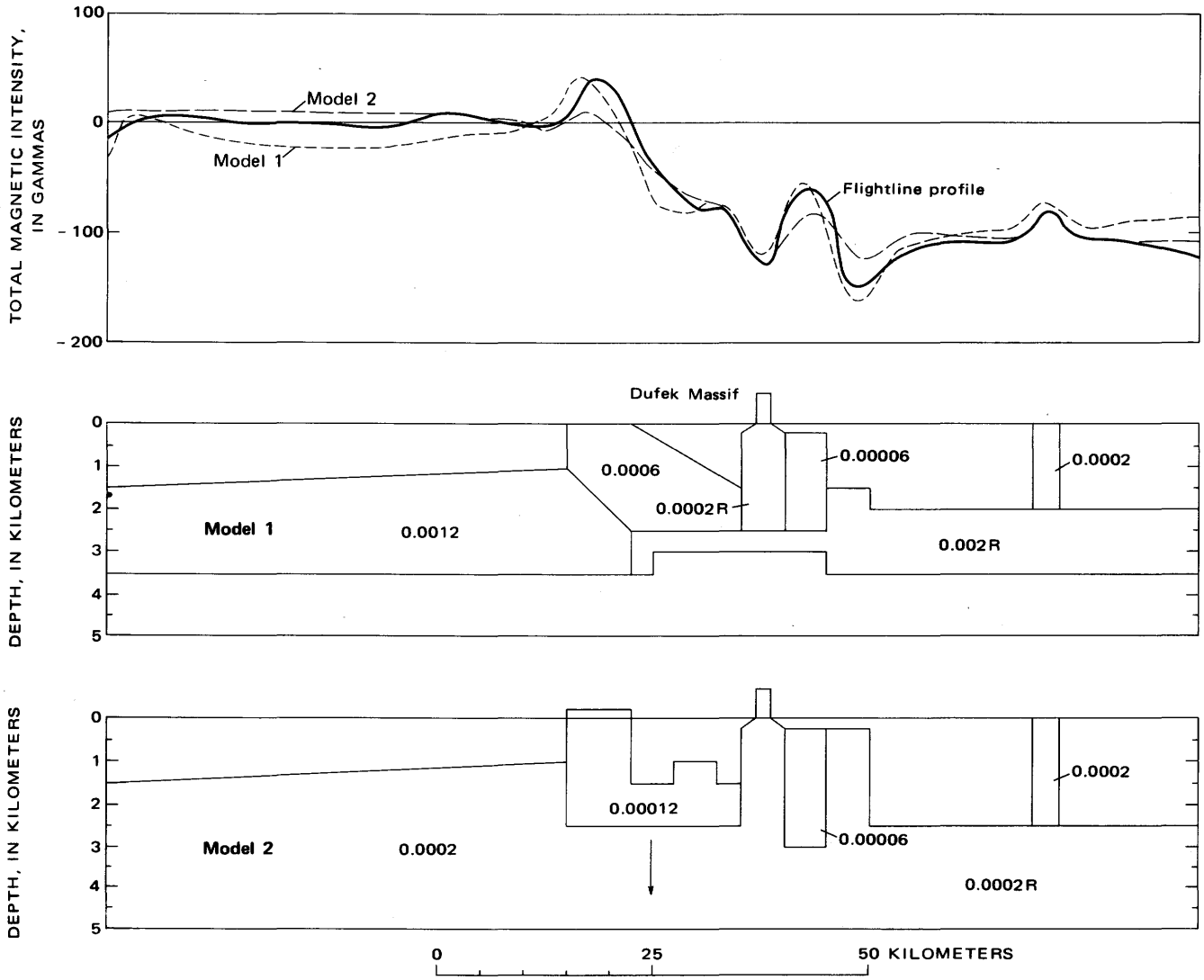

FIGURE 16. — Magnetic profile along line 26 (pl. 2*C*). Theoretical profiles were computed for indicated models. Arrow in model 2 indicates extension of body to infinite depths. Magnetizations are indicated in emu/cm³; all inclinations of magnetization are 70°; R refers to body having reversed magnetization.

depth below the lowest exposed part of the intrusion (with possibly a gradational decrease in magnetization) or that magnetization is higher in a thin layer at the base of the section below the measured samples in the exposed rocks. Note that these models require some reversed polarization of magnetization to fit the observed data. A possible geologic explanation for the existence of a layer having a higher magnetization at the base of the intrusion (model 1) would be the presence of an ultramafic layer there; ultramafic layers at the base of other mafic intrusions, for example the Stillwater Complex in Montana (Howland, 1955, p. 103–105), have associated high-amplitude magnetic anomalies (U.S. Geol. Survey, 1971).

Plate 2*A* illustrates the lower amplitude magnetic anomalies in the Pensacola Mountains magnetic survey. The data in the area over the ice sheet on lines 1–31 northwest of the Dufek Massif and lines 1–37 southeast of the Forrestal Range show several anomalies of 100–200 gammas amplitude. Comparison of these data flown at an elevation of 2,100 m with the bedrock elevations in figure 3 and the seismic depths on plate 1 shows that high magnetizations are required in the rock masses producing these anomalies. We interpret these rock masses as probable extensions of the Dufek intrusion northwest of the Dufek Massif and southeast of the Forrestal Range. There is some support for this interpretation in the gravity data, as discussed previously. The positive Bouguer anomaly of the seismic reflection station near 83°30′ S., 45° W., correlates approximately with positive magnetic anomalies at the east ends of lines 26 and 31. The positive Bouguer anomalies at two seismic stations in the area near 81°30′ S., 55° W., correlate with positive magnetic anomalies at the northwest ends of lines 11 and 16 and with the magnetic data along the Filchner Ice Shelf Traverse (fig. 13).

Figure 13 was compiled from magnetic data observed in 1963–64 (Behrendt, 1964) and from vertical intensity data observed on the Filchner Ice Shelf Traverse of 1957 (Behrendt, 1961). Because this map covers such a large area, it was necessary to remove the regional gradient. Only anomalies along the profiles are indicated. The high-amplitude anomalies in the Dufek Massif and Forrestal Range area (flight W3 in fig. 13) were the first ones recorded over the Dufek intrusion; they offered the first evidence of the fact that the anomalies over the Forrestal Range are comparable with those over the Dufek Massif (Behrendt, 1964) and that rocks in the Forrestal Range are part of the Dufek intrusion. Figure 13 bears on the question of the possible extent of the Dufek intrusion outside the area of the Pensacola Mountains survey (as indicated on pl. 2) and contains the only known magnetic data in this area. Comparison of anomalies A and B in figure 13 with the anomalies on plate 2 over the Forrestal Range and Dufek Massif (and the trend indicated for these anomalies) suggests that anomalies A and B may be extensions of the anomalies over the Dufek intrusion and that the rocks causing them are possibly part of this intrusion. The Filchner Ice Shelf Traverse data across Berkner Island and extending south to the Dufek Massif show that continuous high-amplitude anomalies occur all along this section. The amplitudes observed at 900 m above the rocks on flight W3 over the Forrestal Range and Dufek Massif (fig. 13) are very high and have a peak-to-trough range of the order of 1,500 gammas, whereas anomalies A and B are only about 200 gammas. Figure 13, because of the compressed horizontal scale and expanded vertical scale compared with scales on plate 2, amplifies the anomalies.

Figure 17 shows anomalies over the Dufek Massif and Forrestal Range continued upward (using the method of Henderson, 1960) to various levels for comparison with anomaly B (fig. 13), which was observed at elevations from 1,200 m to perhaps 1,500 m or more above the bedrock. Profile B1 shows anomaly B at the same vertical scale as profile 11; B2 shows anomaly B at an expanded vertical scale. We do not know the depth to the source of anomaly B, but it certainly is less than 6–9 km, which were the approximate depths required to reduce the anomaly to about 200 gammas amplitude, shown on profile 11 over the Dufek Massif and Forrestal Range. Profile B2 suggests sources of only a few kilometers depth. Comparison of the upward continued profiles and profile B1 indicates that the high magnetizations used to fit profile 11 (fig. 14) are not present at depth in the area of anomaly B. Therefore we conclude that if anomalies A and B are a continuation of the anomalies over the Dufek intrusion, they must be from lower parts of the intrusion and are similar to anomalies in the southern Dufek Massif indicated on plate 2 and in figure 16.

The area of the intrusion is about 24,000 km², as estimated on the basis of the extent of the anomalies shown on plate 2 that we have interpreted as associated with the Dufek intrusion, but not including anomalies outside the Pensacola survey, such as A, B, and others in figure 13. If we include the areas interpreted from the gravity data of plate 1 as associated with the Dufek intrusion outside the area of the magnetic survey, we obtain an additional areal extent of approximately 10,000 km². Therefore, within the area of the Pensacola Mountains geophysical survey, an area of about 34,000 km² is underlain by rocks that are part of the Dufek intrusion. This area is about half the size of the Bushveld mafic complex (Hamilton, 1970). We cannot establish the northward extent of the Dufek intrusion beyond the area of the Pensacola Mountains survey on the basis of the data in figure 13, although these data suggest that the intrusion could continue to anomalies A and B. Additional systematic surveys are needed to answer this very important question.

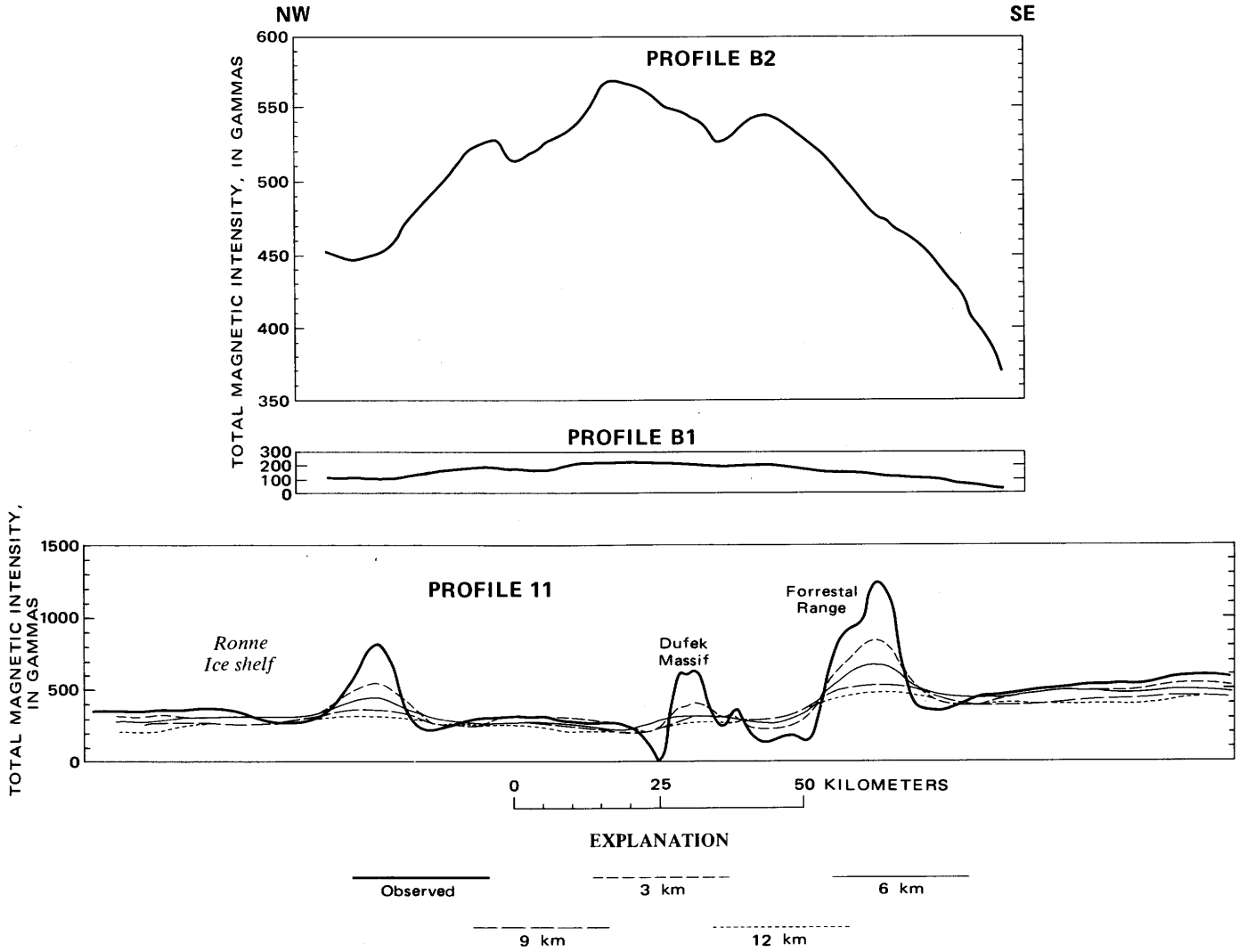

FIGURE 17. — Upward continuation of magnetic profile along line 11 (pl. 2*C*). Profiles across anomaly B in figure 13 are indicated on two scales; profile B1 has same scale as profile 11.

NEPTUNE AND PATUXENT RANGES

For the Neptune and Patuxent Ranges, south of the area of the Dufek intrusion, the lower amplitude magnetic anomalies are shown on plate 2. Compared with the area of the Dufek intrusion, the area of the Neptune Range (pl. 2*B*) is fairly smooth and featureless, but plate 2*A* (the "high gain" display) shows many anomalies over the Neptune and Patuxent Ranges in the range of 50–200 gammas. We interpret the approximately 50-gamma-amplitude anomalies on lines 36 through 39 in the Schmidt Hills area (pl. 2*A*) to be associated with the Precambrian diabase intrusions mapped by Schmidt and Ford (1969). Although their map does not show any diabase intrusions in the Patuxent Formation in the south end of the Patuxent Range, profiles 48 and 49 near Snake Ridge have anomalies that are similar to those over the Schmidt Hills, suggesting the presence of diabase intrusions buried by ice in this area. A 200-gamma negative anomaly crossing Weber Ridge at the north end of the Patuxent Range correlates with a positive Bouguer anomaly shown on plate 1, although the gravity data are sparse or lacking in most of the area crossed by the magnetic anomaly. We interpret this anomaly source as a mafic intrusion, probably very magnetic, which may have been intruded at a time of reversed magnetic-field polarity. A similar magnetic anomaly, which probably has a similar origin, can be seen at the northwest end of line 50 over the ice sheet. This anomaly has about the same amplitude as anomaly C in figure 13 but is of opposite sign. Several anomalies of about 100 gammas occur near the east ends of the profiles from line 43 north over the ice sheet to the area of inferred Dufek intrusion. One of these near the east end of line 42 is negative, suggesting reversed magnetization. We do not know whether there is any association between these features, which are probably caused by mafic rocks of either intrusive or extrusive origin, and the Dufek intrusion.

OTHER MAGNETIC ANOMALIES

Generally the profiles over the sedimentary rocks in the Pensacola Mountains are of low amplitude compared with those in the surrounding areas (fig. 13). We interpret the broad flat area in the vicinity of the seismic reflection profile near 83° S., 70° W. (fig. 13), as indicative of a thick section of sedimentary rock. The low mean crustal velocity of 6 km/s reported by Manfred Hochstein (Bentley, 1973) in this area and the negative gravity anomaly along profile $A-A'$ in this area on plate 1 support this interpretation. The observed data do not show any anomalies as large as 10 gammas on flightlines W3, WR2, and WR1 in this area. Comparison of this magnetically quiet area with anomaly B as shown by profile B1 (fig. 17) illustrates the flatness of the field in the quiet area. By contrast, high-amplitude anomalies occur throughout the rest of the area of figure 13. Considering that the flight elevation, although variable throughout the area of figure 13, was generally several thousand meters above the ice-covered rock surface and consequently much higher above the rocks than the survey data over the Pensacola Mountains shown on plate 2, the rocks must have high magnetizations to produce the observed anomalies. We can only speculate on the origins of these anomalies inasmuch as the area, as indicated in figure 13, is covered with ice.

Craddock (1970a) reported volcanic bedrock in the southern Ellsworth Mountains. He reported mafic lava flows at three locations in the Heritage Range of the Ellsworth Mountains which may be the source of the numerous magnetic anomalies in the southern Heritage Range (fig. 13). Craddock (1970a) showed Cenozoic intrusive rocks (mainly felsic in composition), Paleozoic and Paleozoic(?) sedimentary rocks, and Paleozoic(?) intrusive rocks in the Hart Hills (gabbro), and Precambrian metasedimentary rocks in the outcrops near 84° S., 90° W. The gabbro in the Hart Hills probably is the source of the anomalies there. Perhaps some of these mafic rock types, which would likely contain substantial amounts of magnetite in either extrusive or intrusive form, are the sources of the anomalies in the areas beneath the ice sheet shown in figure 13.

DISCUSSION

The concept of Antarctica as a part of Gondwanaland is now generally accepted. The exact configuration of Antarctica in relation to the other southern hemisphere continents, however, remains open for discussion, and the evidence from Antarctica for and against a number of postulated fittings was discussed by Ford (1972). For example, Craddock (1970b) presented a reconstruction that is generally acceptable to many geologists (fig. 18). We do not understand completely the tectonic history of the Pensacola Mountains and their relation to the Transantarctic Mountains in the breakup of Gondwanaland. The gravity data presented in this report and those shown by Robinson (1964) and Behrendt and Bentley (1968) for all of Antarctica show a generally steep gradient increasing from West to East Antarctica roughly coincident with the front of the Transantarctic Mountains (Ross orogen in fig. 18). Model 3 in figure 11 suggested a fault separating East and West Antarctica, and this interpretation was also made for the data in the McMurdo area by Robinson (1964). Craddock's Andean orogenic belt contains upper Paleozoic and younger rocks. The older rocks in this area are pre-Jurassic (Craddock, 1970a) and Paleozoic. The rocks in the Ellsworth orogenic belt (fig. 18) are partly of early Mesozoic age; our magnetic data indicate numerous anomalies caused by intrusive bodies, some of which could be of the same age. The Dufek intrusion falls into this age range.

The Ross orogeny occurred in early Paleozoic time and affected the Cambrian and Precambrian rocks in the Pensacola Mountains. It is tempting to speculate that the intrusion of the Jurassic diabase into Beacon rocks (Devonian to Jurassic) and the emplacement of the Dufek intrusion in Jurassic time were associated with the tectonic activity that accompanied the separation of Antarctica from Africa. The northward extent of the Dufek intrusion is unknown, as discussed earlier in this report. If the breakup of Gondwanaland took place after the Dufek gabbro was intruded (about 168 m.y. ago), parts of this intrusion might be found in South Africa. As far as we have been able to determine, however, none of the intrusion is present there, which would be consistent with the breakup at the time of, or prior to, the intrusion of the Dufek gabbro. The deep crustal fault suggested by the gravity data bounding East Antarctica occurs along the area of the Jurassic diabase intrusions, and it is probably not fortuitous that the Dufek intrusion and the consequent gravity anomaly are superimposed on the regional gradient associated with the suggested crustal fault. Probably these intrusions and the crustal fault are syntectonic. If the boundary between East and West Antarctica originated at the time of separation of Antarctica from Gondwanaland, the West Antarctica crust in the area of the Pensacola Mountains may be younger and consequently thinner than normal. Therefore, the 24-km thickness measured by Manfred Hochstein (Bentley, 1973) may be realistic. If it is, the linear gravity gradient along the boundary between East and West Antarctica would not imply a near-vertical fault at the crust-mantle boundary, and model 1 in figure 11 would be most representative of the actual structure.

The magnetic model in figure 14 shows downfaulted rocks northwest of the Dufek Massif, whereas the gravity models in figure 11 show an upfaulted block on the northwest side of the Pensacola Mountains. This difference implies that these two faults are not the same age, which is consistent with our suggestion that rifting of Gondwanaland and intrusion of the Dufek gabbro took place at approximately the same time. Schmidt and Ford (1969)

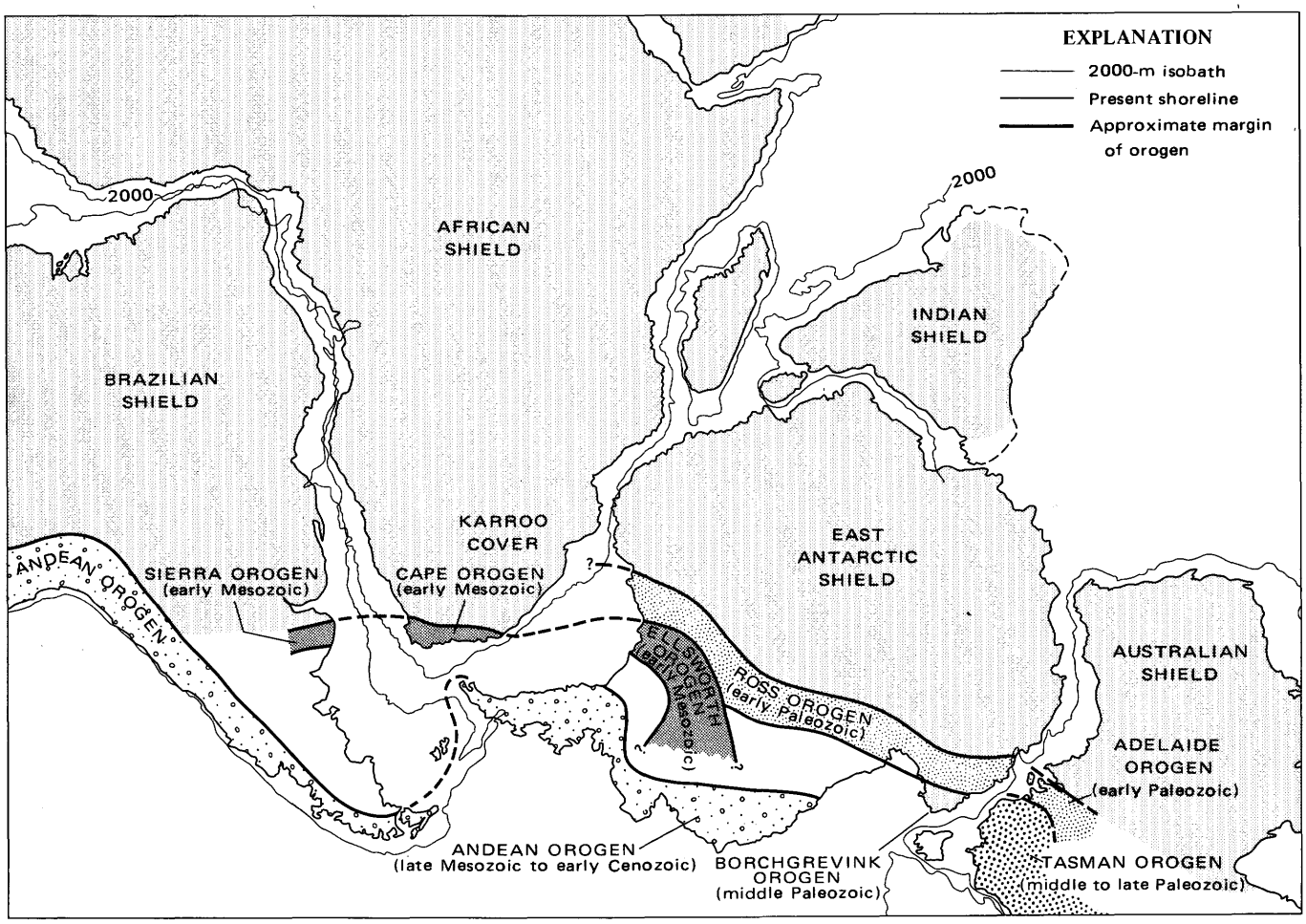

FIGURE 18. — Reconstruction of Gondwanaland. Modified from Craddock (1970b).

suggested a fairly young age for the faulting at the northwest side of the Dufek Massif. Possibly the topographically low area between the Thiel Mountains and the Patuxent Mountains, indicated by closed bedrock-elevation contours in figure 3 and by seismic reflection data on plate 1, has a tectonic origin and is contemporaneous with faulting which uplifted the block of the Pensacola Mountains. Although thick basins containing Tertiary sedimentary rocks are not known in Antarctica, one would expect them to border ranges such as the Pensacola Mountains and to be covered by the ice sheet. Such basins would account for the low seismic crustal velocity observed at the reflection station (R on pl. 1 and in fig. 13), the magnetically quiet area northwest of the Patuxent Range, and the apparent negative gravity anomaly discussed previously in relation to the crustal reflection models in figure 11. Certainly the activity that resulted in the Pensacola Mountains being uplifted 4 km relative to the rocks northwest of the ranges must have occurred in Pliocene or Pleistocene time for the relief to have been maintained to the present.

The magnetic models in figure 17 suggest a layer with higher magnetism at the base of the Dufek Massif. This higher magnetism could be an indication of an ultramafic layer, and if so, one might expect a conductivity anomaly that could be detected by electromagnetic soundings.

The most useful approach for future geophysical work in the Pensacola Mountains appears to be additional aeromagnetic traverses combined with radar ice-thickness soundings to determine the northern extent of the Dufek intrusion and the configuration of the bedrock surface beneath the ice sheet. Radar echo soundings would not penetrate sea water beneath the ice shelf, but magnetic data observed on closely spaced lines would delineate the northern boundary of the intrusion.

Additional gravity work in the Pensacola Mountains would not be productive unless large-scale (1 : 62,500) topographic maps sufficient for terrain corrections are available; radar echo sounding of the ice-covered area surrounding the ranges is required for terrain corrections of stations on bedrock adjacent to the ice. Additional gravity data in the ice-covered area shown on plate 1 would be very useful on a regional basis if ice-thickness measurements of some type were made at the exact sites to allow the construction of a more accurate regional gravity map. This

would allow a comparison of regional data with the data over the Dufek intrusion and a better isolation of the anomaly associated with this intrusion than indicated in figure 12.

SUMMARY AND CONCLUSIONS

In this report we have discussed the interpretations of the geophysical surveys in relation to the geology of the Pensacola Mountains. The gravity and magnetic data indicate several features. There is a broad regional Bouguer anomaly that decreases from West to East Antarctica and has a 4-mgal/km gradient in the steepest areas. Values range from 82 mgal on the West Antarctica side to −90 mgal in the center of the Pensacola Mountains. Theoretical profiles fitted to the observed gravity data across the Pensacola Mountains front in the vicinity at the Patuxent Range indicate either of two structural configurations: (1) an abnormally thin crust on the West Antarctica side of perhaps 24 km, as suggested by a deep seismic reflection reported by Manfred Hochstein (Bentley, 1973), or (2) a normal crust on the West Antarctica side and a steep steplike transition from West to East Antarctica that suggests a fault extending from the crust-mantle boundary to, perhaps, the surface in the vicinity of the Schmidt Hills. Gravity, magnetic, and seismic data on the West Antarctica side of this profile suggest a thick section of low-velocity, low-density, nonmagnetic, presumably sedimentary rock.

A least-squares regression of the Bouguer anomalies compared with elevation in the Pensacola Mountains area suggests that the amplitude of the gravity anomaly over the Dufek intrusion is about 85 mgal, which would correspond to a thickness of about 8.8−6.2 km for the total section of the Dufek intrusion, using a reasonable range of density contrast. Magnetic anomalies of about 2,000 gammas from peak to trough are associated with the intrusion. The amplitudes are highest in the Forrestal Range and decrease in the Dufek Massif from north to south. This range in amplitudes is consistent with measured magnetic properties and computed theoretical magnetic models. The computed magnetic models fitted to high-amplitude anomalies on profiles crossing the upper and middle parts of the section in the Dufek Massif and Forrestal Range show normal and reversed magnetizations of the same order of magnitude as those measured from surface samples. Models fitted to 100- to 200- gamma anomalies observed on profiles over the lower part of the section in the southern Dufek Massif require either a basal unexposed layer, 1−2 km thick, of a magnetization higher than that measured from the lowest exposed rocks, or infinitely thick bodies of observed low magnetization. The second hypothesis is geologically unreasonable; the first suggests a possible basal ultramafic layer.

Both magnetic and gravity data suggest an extension of the Dufek intrusion beneath the ice. The magnetic data indicate a minimum areal extent of about 24,000 km²; gravity data beyond the area of the magnetic survey suggest an additional 10,000 km², giving a total minimum estimate of 34,000 km². Other magnetic data to the north and west of the Pensacola Mountains survey suggest a possible continuation of the Dufek intrusion as far north as 250 km, underlying Berkner Island, but this interpretation requires further investigation. If the anomalies in the Berkner Island area are associated with the Dufek intrusion, the highly magnetic rocks of the type observed in the upper section in the Forrestal Range are probably missing.

The free-air-anomaly map and profiles and the Bouguer anomaly−elevation regression calculation suggest that the area of the Pensacola Mountains is in regional isostatic equilibrium.

Smaller amplitude gravity and magnetic anomalies exist throughout the area. Gravity anomalies include a 10- to 20-mgal positive Bouguer anomaly in the southern Neptune Range, a 20- to 30- mgal negative anomaly over Paleozoic rocks relative to Precambrian sedimentary rocks, a −30-mgal anomaly over the granite of Median Snowfield in the Washington Escarpment area, and a +20-mgal anomaly in the northern Patuxent Range. The gravity anomaly in the northern Patuxent Range correlates with a negative magnetic anomaly in the same area, which we have interpreted as a mafic intrusive body with reversed magnetization. Magnetic anomalies are associated with known diabase intrusions in the Schmidt Hills, and similar anomalies in the southern Patuxent Range suggest the presence of unexposed diabase intrusions. A −200-gamma anomaly near the southwest corner of the surveyed area and a negative anomaly east of the southern Neptune Range suggest reversed remanent magnetization in rocks beneath the ice sheet. A compilation of previous magnetic traverses throughout the area indicates numerous magnetic anomalies of about 100−300 gammas and suggests that the rocks in the Pensacola Mountains have anomalously low magnetizations compared with those in the rest of the area with the exception of a very flat magnetic field, mentioned previously, northwest of the Pensacola Mountains.

REFERENCES

Aughenbaugh, N. B., 1961, Preliminary report on the geology of the Dufek Massif, *in* Reports of Antarctic geological observations, 1956−1960: Am. Geog. Soc., Internat. Geophys. Year World Data Center A, Glaciology, IGY Glaciological Rept. Ser. 4, p. 155−193.

Beck, M. E., Jr., and Griffin, N. L., 1971, Magnetic intensities in a differentiated gabbroic body, the Dufek intrusion, Pensacola Mountains, Antarctica, *in* Geological Survey research 1971: U.S. Geol. Survey Prof. Paper 750−B, p. B117−B121.

Behrendt, J. C., 1961, Geophysical studies in the Filchner ice shelf area of Antarctica: Wisconsin Univ. Ph. D. thesis, 191 p.

———1962a, Geophysical and glaciological studies in the Filchner ice shelf area of Antarctica: Jour. Geophys. Research, v. 67, no. 1, p. 221−234.

———1962b, Summary and discussion of the geophysical and glaciological work in the Filchner ice shelf area of Antarctica: Wisconsin Univ. Geophys. and Polar Research Center Research Rept. Ser. 62−3, 66 p.

———1964, Distribution of narrow-width magnetic anomalies in Antarctica: Science, v. 144, no. 3621, p. 993–999.

Behrendt, J. C., and Bentley, C. R., 1968, Magnetic and gravity maps of the Antarctic: Am. Geog. Soc. Antarctic Map Folio Ser. 9.

Behrendt, J. C., Meister, Laurent, and Henderson, J. R., 1966, Airborne geophysical study in the Pensacola Mountains of Antarctica: Science, v. 153, no. 3742, p. 1373–1376.

Behrendt, J. C., Wold, R. J., and Laudon, T. S., 1962, Gravity base stations in Antarctica: Royal Astron. Soc. Geophys. Jour., v. 6, no. 3, p. 400–405.

Bentley, C. R., 1964, The structure of Antarctica and its ice cover, chap. 14 *in* Odishaw, Hugh, Solid earth and interface phenomena: Research in geophysics, Cambridge, Mass., M.I.T. Press, v. 2 p. 335–389.

———1973, Crustal structure of Antarctica, *in* Crustal structure based on seismic data, IUMC Proc. — A symposium: Tectonophysics (in press).

Craddock, Campbell, compiler, 1970a, Geologic map of Antarctica [entire continent], *in* Bushnell, V. C., and Craddock, Campbell, eds., Geologic maps of Antarctica, 1969–70: Am. Geog. Soc. Antarctic Map Folio Ser. 12, pl. 20.

———1970b, Map of Gondwanaland, *in* Bushnell, V. C., and Craddock, Campbell, eds., Geologic maps of Antarctica, 1969–70: Am. Geog. Soc. Antarctic Map Folio Ser. 12, pl. 23.

Daly, R. A., 1933, Igneous rocks and the depths of the earth [2d ed.]: New York and London, McGraw-Hill Book Co., 598 p.

Ford, A. B., 1970, Development of the layered series and capping granophyre of the Dufek intrusion of Antarctica, *in* Bushveld igneous complex and other layered intrusions — A symposium: Geol. Soc. South Africa Spec. Pub. 1, p. 492–510.

———1972, Fit of Gondwana continents — Drift reconstruction from the Antarctic continental viewpoint: Internat. Geol. Cong., 24th, Montreal, 1972, Proc., Sec. 3, p. 113–121.

———1973, The Weddell orogeny — Latest Permian to early Mesozoic deformation at the Weddell Sea margin of the Transantarctic Mountains: Symposium on geology and solid earth geophysics of Antarctica, Oslo, Norway, 1970, Proc., p. 419–425.

Ford, A. B., and Boyd, W. W., Jr., 1968, The Dufek intrusion, a major stratiform gabbroic body in the Pensacola Mountains, Antarctica: Internat. Geol. Cong., 23d, Prague, 1968, Proc., Sec. 2, Volcanism and tectogenesis, v. 2, p. 213–228.

Hamilton, Warren, 1970, Bushveld complex — product of impacts? *in* Busheveld igneous complex and other layered intrusions — A symposium: Geol. Soc. South Africa Spec. Pub. 1, p. 367–374.

Henderson, R. G., 1960, A comprehensive system of automatic computation in magnetic and gravity interpretation: Geophysics, v. 25, no. 3, p. 569–585.

Howland, A. L., 1955, Chromite deposits in the central part of the Stillwater complex, Sweet Grass County, Montana: U.S. Geol. Survey Bull. 1015–D, p. 99–121.

Huffman, J. W., and Schmidt, D. L., 1966, Pensacola Mountains Project: Antarctic Jour. U.S., v. 1, no. 4, p. 123–124.

Neuburg, H. A. C., Thiel, E., Walker, P. T., Behrendt, J. C., and Aughenbaugh, N. B., 1959, The Filchner Ice Shelf: Assoc. Am. Geographers Annals, v. 49, no. 2, p. 110–119.

Robinson, E. S., 1964, Geological structure of the Transantarctic Mountains and adjacent ice covered areas, Antarctica: Wisconsin Univ. Ph. D. thesis, 319 p.

Schmidt, D. L., Dover, J. H., Ford, A. B., and Brown, R. D., 1964, Geology of the Patuxent Mountains, *in* Adie, R. J., ed., Antarctic geology — Internat. symposium on Antarctic geology, 1st, Cape Town, 1963, Proc.: Amsterdam, North-Holland Publishing Co., p. 276–283.

Schmidt, D. L., and Ford, A. B., 1969, Geologic map of Antarctica — Pensacola and Thiel Mountains, *in* Bushnell, V. C., and Craddock, Campbell, eds., Geologic maps of Antarctica 1969–70: Am. Geog. Soc. Antarctic Map Folio Ser. 12, pl. 5

Schmidt, D. L., Williams, P. L., Nelson, W. H., and Ege, J. R., 1965, Upper Precambrian and Paleozoic stratigraphy and structure of the Neptune Range, Antarctica, *in* Geological Survey research 1965: U.S. Geol. Survey Prof. Paper 525–D, p. D112–D119.

Thiel, Edward, and Behrendt, J. C., 1959, Seismic studies on the Filchner Ice Shelf, Antarctica, 1957–1958, *in* Oversnow traverse programs, Byrd and Ellsworth stations, Antarctica, 1957–1958 — Seismology, gravity, and magnetism: Am. Geog. Soc., Internat. Geophys. Year World Data Center A, Glaciology, IGY Glaciological Rept. Ser. 2, p. V1–V14.

Thiel, Edward, and Ostenso, N. A., 1961, Seismic studies on Antarctic ice shelves: Geophysics, v. 26, no. 6, p. 706–715.

Thiel, E., Ostenso, N. A., Bennett, H. F., Robinson, E. S., and Behrendt, J. C., 1958, IGY Antarctic oversnow traverse program, 1957–1958, *in* Preliminary reports of the Antarctic and northern hemisphere glaciology programs: Am. Geog. Soc., Internat. Geophys. Year World Data Center A, Glaciology, IGY Glaciological Rept. Ser. 1, p. 11–114.

U.S. Geological Survey, 1971, Aeromagnetic map of the Stillwater complex and vicinity, south-central Montana: U.S. Geol. Survey open-file map.

Williams, P. L., 1969, Petrology of upper Precambrian and Paleozoic sandstones in the Pensacola Mountains, Antarctica: Jour. Sed. Petrology, v. 39, no. 4, p. 1455–1465.

Wold, R. J., 1964, The Elsec Wisconsin digital recording proton precession magnetometer system: Wisconsin Univ. Geophys. and Polar Research Center Research Rept. Ser. 64–4, 83 p.

Woollard, G. P., 1962, Geologic effects in gravity values, pt. 3 *of* the relation of gravity anomalies to surface elevation, crustal structure and geology: Wisconsin Univ. Geophys. and Polar Research Center Research Rept. Ser. 62–9, 78 p.

TABLE 2

TABLE 2. — Data from gravity reduction program, Camp Neptune, Pensacola Mountains

Sta.	Lat[2]	Long[3]	Elev[4]	Obs G[5]	FAA[6]	BA[7]
1	83 7.87	56 57.67	978.0	4969.54	124.03	14.59
2	83 4.53	55 13.77	1136.0	4872.58	76.97	-50.16
3	83 7.21	54 45.53	1187.0	4857.21	76.35	-56.48
4	83 17.28	55 55.61	1118.0	4881.39	75.69	-49.42
5	83 26.86	55 59.60	1209.0	4874.78	93.80	-41.49
6	83 32.21	56 36.49	1194.0	4859.45	72.02	-61.59
7	83 36.73	56 51.05	953.0	4909.50	46.28	-60.36
8	84 3.04	57 2.47	1405.0	4821.52	89.10	-68.12
9	83 57.77	55 26.09	1630.0	4765.70	104.26	-78.14
10	83 45.16	57 7.63	1164.0	4859.52	58.54	-71.71
11	83 42.11	56 9.20	1246.0	4864.74	90.03	-49.40
13	83 33.75	55 53.17	1346.0	4835.71	94.61	-56.02
14	83 27.31	53 29.15	1524.0	4746.77	62.70	-107.84
16	83 29.10	54 16.20	1232.0	4832.66	58.00	-79.86
17	83 34.90	54 26.90	1433.0	4810.52	95.84	-64.52
18	83 29.29	51 16.38	1450.0	4798.60	91.05	-71.21
19	83 14.10	50 55.20	1995.0	4738.51	174.15	-49.10
20	83 33.90	54 56.10	1279.0	4849.16	87.36	-55.77
21	83 25.70	51 23.00	1414.0	4807.25	89.84	-68.39
22	83 27.30	51 23.10	1431.0	4803.48	90.76	-69.38
23	83 23.70	51 47.30	1510.0	4797.01	109.87	-59.11
24	83 5.07	50 33.83	1658.0	4760.76	125.80	-59.73
25	83 20.10	55 59.30	1025.0	4908.23	72.88	-41.82
26	83 8.23	49 5.94	1617.0	4805.01	156.28	-24.67
27	82 44.28	48 9.53	1028.0	4947.45	126.05	11.01
28	82 40.63	49 1.92	1146.0	4897.36	113.72	-14.52
29	83 12.20	51 26.90	1397.0	4805.15	87.22	-69.11
30	83 56.60	56 19.30	1037.0	4921.18	77.38	-38.66
31	84 0.70	56 3.00	1380.0	4831.82	92.43	-62.00
32	83 59.70	56 31.40	1308.0	4857.77	96.51	-49.86
33	84 15.07	60 25.02	767.0	4844.76	-87.97	-173.80
34	84 25.40	63 34.53	1017.0	4920.74	62.00	-51.81
35	84 22.44	63 20.01	870.0	4963.33	60.15	-37.20
36	84 24.28	62 48.65	787.0	4977.22	47.92	-40.15
37	84 31.84	64 53.73	1073.0	4906.45	63.10	-56.97
38	84 31.90	63 39.10	816.0	4969.36	46.79	-44.53
39	84 40.50	64 25.10	919.0	4949.98	56.72	-46.12
40	83 39.56	61 23.76	310.0	4942.17	-120.20	-154.89
41	83 43.40	65 29.00	489.0	5024.92	16.47	-38.25
42	83 41.50	64 45.70	401.0	5041.40	6.44	-38.43
43	83 40.10	63 57.50	335.0	4993.10	-61.74	-99.23
44	83 38.70	63 9.50	336.0	4954.80	-99.27	-136.87
45	83 37.30	62 22.40	330.0	4943.21	-112.24	-149.17
46	83 34.10	60 48.80	299.0	4946.23	-117.71	-151.17
47	83 40.30	58 42.20	893.0	4935.58	52.68	-47.25
48	83 53.70	55 36.50	1472.0	4810.79	111.96	-62.76
49	83 54.90	55 33.10	1511.0	4797.20	100.01	-69.08
50	83 55.30	55 9.10	1497.0	4798.84	97.21	-70.31
51	83 54.19	54 53.65	1615.0	4765.25	100.33	-80.39
52	83 57.10	54 27.00	1450.0	4817.45	100.76	-61.50
53	83 49.70	56 28.20	1311.0	4860.58	103.43	-43.28
54	82 46.04	53 23.53	1138.0	4858.48	70.32	-57.03
55	83 48.96	66 13.26	963.0	4971.78	107.62	-0.14
56	83 58.60	66 26.60	850.0	4987.66	85.59	-9.53
57	84 3.50	66 6.20	677.0	5008.09	51.16	-24.60
58	84 5.60	66 8.70	619.0	5005.40	29.94	-39.33
59	84 6.60	66 34.50	731.0	4982.48	41.24	-40.56
60	84 20.40	64 55.30	916.0	4953.15	64.75	-37.75
61	84 18.70	64 36.80	693.0	5001.95	45.32	-32.23
62	84 21.80	64 30.80	753.0	4987.75	48.70	-35.57
63	84 16.80	62 54.50	438.0	5066.09	31.42	-17.59
64	83 48.60	58 55.50	611.0	4978.05	5.51	-62.86
65	83 45.01	58 52.50	1136.0	4887.79	78.23	-48.89
66	83 48.70	53 25.00	1425.0	4745.11	23.41	-136.05
67	83 50.80	52 42.10	1418.0	4791.55	67.02	-91.66
68	83 52.70	51 58.70	1299.0	4802.60	40.79	-104.58
69	83 54.70	51 15.20	1267.0	4763.96	-8.36	-150.14
70	83 58.40	49 46.00	1234.0	4722.67	-60.99	-199.08
71	84 0.10	48 59.70	1242.0	4743.85	-37.88	-176.86
72	84 1.80	48 12.80	1250.0	4750.32	-29.48	-169.36
73	84 3.40	47 24.80	1237.0	4766.31	-17.99	-156.42
74	83 29.64	65 13.50	513.0	5024.31	27.86	-29.55
75	83 31.80	64 27.90	468.0	5022.08	11.02	-41.35
76	83 33.80	63 42.50	422.0	5066.42	40.51	-6.72
77	83 35.80	62 56.10	313.0	5015.24	-44.95	-79.98
78	84 9.90	46 2.40	1338.0	4779.01	23.83	-125.90
79	84 17.60	42 54.50	1495.0	4767.40	58.27	-109.03
80	84 15.80	43 41.80	1454.0	4754.22	32.99	-129.71
81	84 13.90	44 29.20	1420.0	4763.98	32.85	-126.05
82	84 11.90	45 16.10	1377.0	4775.23	31.46	-122.64
83	83 34.20	57 28.20	611.0	4954.28	-13.51	-81.88
84	83 34.50	57 32.50	602.0	4959.08	-11.58	-78.95
85	83 34.70	57 36.30	578.0	4966.38	-11.75	-76.43
86	83 34.90	57 40.00	557.0	4968.95	-15.72	-78.05
87	83 35.20	57 43.10	564.0	4962.62	-19.99	-83.10
88	83 35.50	57 47.20	567.0	4959.55	-22.24	-85.69
89	83 35.70	57 50.30	564.0	4959.28	-23.50	-86.61
90	83 35.90	57 54.00	561.0	4956.49	-27.28	-90.06
91	83 36.20	57 57.20	553.0	4952.09	-34.25	-96.13
92	83 36.40	58 0.60	540.0	4946.51	-43.90	-104.33
93	83 36.60	58 4.40	537.0	4936.14	-55.26	-115.35
94	83 36.90	58 8.20	534.0	4923.24	-69.19	-128.94
95	83 37.10	58 11.90	534.0	4912.40	-80.09	-139.85
96	83 37.40	58 15.10	539.0	4904.28	-86.77	-147.09
97	83 37.70	58 19.20	550.0	4898.88	-88.88	-150.43
98	83 37.90	58 22.70	552.0	4900.41	-86.80	-148.57
99	83 38.20	58 26.80	553.0	4907.99	-79.01	-140.90
100	83 38.40	58 30.30	554.0	4926.24	-62.52	-124.52
101	83 9.70	51 17.60	1435.0	4797.06	91.73	-68.85
102	83 13.10	51 12.90	1475.0	4789.91	95.69	-69.36
103	83 31.60	55 16.70	1249.0	4864.81	96.54	-45.23
104	83 29.80	56 2.50	1056.0	4908.31	79.17	-39.00
105	83 29.51	57 0.72	834.0	4949.24	51.78	-41.55
106	83 28.70	57 30.30	555.0	5015.72	32.53	-29.57
107	82 34.30	47 55.60	794.0	5009.20	119.50	30.65
108	82 40.80	47 44.90	653.0	5007.41	71.75	-1.32
109	82 45.20	48 0.0	638.0	5020.68	78.72	7.33
110	82 45.70	48 14.90	1030.0	4950.59	129.27	14.01
111	83 20.70	49 25.60	1145.0	4868.24	69.66	-58.47
112	83 23.10	49 29.10	1126.0	4887.27	82.00	-44.00
113	83 24.30	49 26.00	1186.0	4859.15	71.96	-60.76
114	83 22.80	50 0.40	1558.0	4804.42	132.38	-41.97
115	83 25.10	50 6.50	1236.0	4851.64	79.58	-58.73
116	83 26.70	50 46.50	1318.0	4837.90	90.56	-56.93
117	83 27.90	51 27.20	1683.0	4745.76	110.48	-77.85
118	82 39.40	44 16.89	338.0	5005.80	-26.43	-64.25
119	82 15.38	41 25.35	878.0	4911.87	55.55	-42.70
120	82 46.92	54 52.05	689.0	4944.91	18.03	-59.08
121	82 27.02	57 16.16	159.0	5031.03	-51.58	-69.37
122	82 8.20	59 21.20	164.0	5039.75	-33.76	-52.11
123	81 51.40	61 19.80	150.0	5053.86	-16.97	-33.75
124	81 54.90	60 57.50	148.0	5049.40	-23.52	-40.08
125	81 58.20	60 34.00	148.0	5046.83	-27.48	-44.04
126	82 1.50	60 10.10	155.0	5046.18	-27.34	-44.69
127	82 4.90	59 45.80	164.0	5041.57	-30.59	-48.94
128	82 11.90	58 57.80	172.0	5027.17	-45.38	-64.63
129	82 15.80	58 33.40	174.0	5026.80	-46.72	-66.19
130	82 19.50	58 8.60	168.0	5030.66	-46.19	-64.99
131	82 23.20	57 42.90	168.0	5045.25	-33.08	-51.88
132	83 3.33	51 52.46	1237.0	4826.46	62.41	-76.02
133	83 34.00	45 4.10	1156.0	4839.54	39.80	-89.56
134	83 47.10	41 5.20	1470.0	4753.16	45.85	-118.65
135	83 31.20	45 47.60	1097.0	4841.63	24.65	-98.10
136	83 28.30	46 31.40	1042.0	4834.14	1.20	-115.40
137	83 25.40	47 13.60	1000.0	4806.60	-38.29	-150.20
138	83 22.40	47 55.20	1012.0	4772.74	-67.42	-180.66
139	83 19.40	48 36.10	984.0	4771.39	-76.35	-186.47
140	83 16.20	49 17.00	987.0	4823.00	-22.70	-133.15
141	83 13.10	49 56.70	1288.0	4858.54	106.70	-37.43
142	83 9.90	50 36.50	1604.0	4784.06	130.73	-48.76
143	83 6.60	51 14.90	1351.0	4781.32	51.22	-99.97
144	82 43.00	55 22.80	521.0	4983.01	5.82	-52.48
145	82 39.10	55 51.80	335.0	5084.10	51.06	13.57
146	82 35.00	56 21.10	158.0	5073.93	-12.10	-29.78
147	83 46.60	55 37.80	1436.0	4824.36	106.73	-53.96
148	83 52.70	56 2.90	1417.0	4823.66	98.21	-60.36
149	83 55.30	56 0.30	1469.0	4814.95	104.69	-59.70
150	83 55.90	56 31.50	968.0	4931.71	66.87	-41.46
151	84 0.30	57 15.90	1182.0	4871.65	71.37	-60.90
152	83 59.79	56 53.09	1137.0	4886.88	72.89	-54.34
153	84 0.0	56 32.90	1301.0	4855.08	91.56	-54.02
154	83 52.80	56 53.70	1113.0	4893.36	74.19	-50.36
155	83 53.60	57 36.90	909.0	4919.75	37.45	-64.27
156	83 58.20	56 44.80	1382.0	4831.47	93.48	-61.17
157	84 00.46	67 1.45	1539.0	4820.08	115.14	-57.08
158	84 51.10	67 14.50	1524.0	4828.22	118.49	-52.05
159	85 37.80	68 42.10	1681.0	4794.03	121.00	-67.11
160	85 8.13	64 54.71	1558.0	4774.12	70.39	-103.96
161	85 22.60	60 54.80	1524.0	4774.44	56.63	-113.91
162	85 35.70	55 47.20	1674.0	4682.97	8.27	-179.06
163	85 40.90	53 4.20	1723.0	4656.73	-4.07	-196.88
164	85 50.70	48 18.40	1845.0	4584.32	-41.07	-247.53
165	84 59.58	66 18.19	1617.0	4802.06	118.72	-62.22
166	85 4.70	71 48.80	1344.0	4772.18	3.39	-147.01
167	83 48.98	57 24.61	1129.0	4866.07	53.06	-73.27
168	83 51.30	57 12.90	1142.0	4881.92	72.17	-55.62
169	83 50.70	56 44.50	1136.0	4896.92	85.52	-41.61
170	83 48.80	56 39.30	982.0	4933.70	75.45	-34.44
171	83 47.60	56 12.30	1259.0	4865.09	92.59	-48.29
172	83 47.20	56 54.90	1086.0	4899.60	73.92	-47.61
173	84 49.10	62 0.0	1192.0	4889.64	78.15	-55.24
174	84 51.78	62 18.93	1659.0	4779.49	111.17	-74.48
175	84 44.70	62 35.60	1000.0	4932.56	63.10	-48.81

TABLE 2. — Data from gravity reduction program, Camp Neptune, Pensacola Mountains[1] — *Continued*

Sta.	Lat[2]	Long[3]	Elev[4]	Obs G[5]	FAA[6]	BA[7]
176	84 46.74	63 24.51	1133.0	4930.11	71.08	-55.71
177	84 48.80	62 59.80	930.0	4951.20	59.04	-45.03
178	84 54.30	62 1.40	1370.0	4842.85	84.81	-68.50
179	84 55.10	62 24.50	1589.0	4804.47	113.69	-64.12
180	84 58.80	62 47.30	1461.0	4835.63	104.43	-59.06
181	84 52.90	63 26.30	1468.0	4797.35	69.88	-94.40
182	85 12.20	78 10.10	1378.0	4713.97	-46.26	-200.46
183	85 13.80	82 54.30	1431.0	4693.99	-50.31	-210.44
184	82 2.80	41 20.30	526.0	4994.43	34.75	-24.11
185	82 5.60	41 3.90	784.0	4933.24	51.93	-35.80
186	82 13.20	42 1.80	381.0	5032.21	23.56	-19.07
187	82 31.10	42 38.50	670.0	4979.34	52.67	-22.31
188	82 36.20	42 45.30	705.0	4970.54	52.68	-26.22
189	83 5.10	54 55.20	1073.0	4879.10	63.86	-56.21
190	83 2.30	50 5.60	1444.0	4840.56	140.67	-20.92
191	83 3.50	50 17.70	1492.0	4817.12	131.58	-35.38
192	83 7.90	50 42.80	1414.0	4813.42	102.26	-55.97
193	83 11.10	50 46.90	1507.0	4792.94	109.29	-59.34
194	83 22.50	50 47.90	2023.0	4728.45	199.77	-26.61
195	83 24.70	50 59.80	1894.0	4723.75	154.57	-57.37
196	82 49.60	48 34.10	1196.0	4929.51	157.88	24.05
197	83 2.30	48 52.80	1022.0	4941.29	111.35	-3.01
198	83 23.90	50 34.60	1730.0	4770.70	151.27	-42.32
199	83 18.90	51 2.10	1916.0	4709.43	149.04	-65.36
500	83 33.95	57 24.68	616.0	4951.40	-14.76	-83.69
501	83 58.41	57 18.32	1453.0	4807.12	90.94	-71.65
502	83 50.74	56 8.86	1396.0	4839.22	107.93	-48.29
503	83 29.98	54 24.75	1674.0	4734.51	95.75	-91.58
504	83 28.40	54 12.30	1386.0	4808.48	81.52	-73.58
505	83 40.40	55 3.00	1594.0	4791.03	124.12	-54.25
506	83 22.94	51 25.00	2066.0	4673.70	158.12	-73.07
507	83 10.80	51 12.10	1447.0	4787.79	85.76	-76.16
508	83 9.20	51 4.60	1399.0	4794.98	78.73	-77.82
509	83 12.40	50 31.20	1783.0	4767.90	168.83	-30.69
510	83 14.23	50 55.51	2028.0	4692.85	168.61	-58.33
511	83 15.90	50 56.60	1988.0	4709.37	172.22	-50.25
512	83 17.40	50 37.90	2025.0	4711.68	185.40	-41.21
513	83 18.90	50 45.10	1526.0	4799.12	118.58	-52.19
514	82 50.25	48 30.62	1251.0	4897.66	142.74	2.75
515	82 55.95	48 28.43	1019.0	4924.81	96.27	-17.76
516	82 52.20	48 11.90	832.0	4959.30	74.52	-18.59
517	83 26.50	53 36.50	1550.0	4765.65	89.87	-83.58
518	83 34.50	53 53.50	1639.0	4747.59	96.52	-86.89
519	83 36.60	53 52.90	1590.0	4760.06	93.18	-84.74
520	83 28.10	54 4.80	1479.0	4785.81	87.61	-77.90
521	83 30.20	54 52.30	1233.0	4856.96	82.23	-55.74
522	83 29.50	55 32.90	1113.0	4897.49	86.02	-38.53
523	82 34.66	48 0.88	910.0	4981.67	127.59	25.76
524	82 31.60	51 11.80	1307.0	4891.22	160.68	14.42
526	83 47.00	55 50.40	1191.0	4883.24	89.98	-43.29
527	84 3.30	54 38.50	1459.0	4808.14	92.28	-70.99
528	84 2.60	56 4.00	1252.0	4863.09	83.66	-56.44
529	84 21.49	62 25.13	762.0	4985.19	49.00	-36.27
530	84 23.64	65 32.79	842.0	4968.33	56.17	-38.06
531	84 17.20	64 7.20	625.0	5018.01	40.87	-29.07
532	84 21.20	65 30.30	758.0	4980.21	42.88	-41.95
533	84 26.70	66 19.80	826.0	4975.60	57.61	-34.82
534	84 38.96	65 56.28	1051.0	4924.06	71.91	-45.70
535	84 37.84	65 25.38	1099.0	4911.86	74.82	-48.16
536	83 23.40	51 44.80	1633.0	4777.17	128.03	-54.71
537	83 22.70	51 42.20	1651.0	4772.77	129.42	-55.33
538	83 21.30	51 43.90	1674.0	4762.88	127.10	-60.23
539	83 19.10	51 30.00	1652.0	4763.96	122.17	-62.70
540	83 16.10	51 22.00	1573.0	4779.01	113.93	-62.09
541	83 19.90	51 14.40	1832.0	4736.22	149.61	-55.40
542	83 25.80	51 47.50	1638.0	4765.69	117.26	-66.03
543	83 25.30	51 47.30	1558.0	4792.97	120.07	-54.28
544	83 24.50	51 44.50	1576.0	4788.66	121.58	-54.78
545	83 28.80	50 38.10	1389.0	4809.26	83.08	-72.35
546	83 38.70	58 34.10	556.0	4953.69	-32.76	-94.97
547	82 36.23	52 21.58	2029.0	4712.93	203.05	-24.01
548	82 29.57	50 53.71	1158.0	4939.05	163.38	33.80
549	82 37.75	52 41.23	1980.0	4689.27	163.70	-57.86
550	82 36.80	52 37.50	1993.0	4702.42	181.23	-41.80
551	82 57.40	54 44.20	950.0	4917.28	66.94	-39.37
552	82 59.50	54 52.60	953.0	4916.18	66.00	-40.65
553	82 35.30	52 44.90	856.0	4969.86	98.89	3.10
554	82 34.70	52 42.60	1007.0	4932.30	108.10	-4.59
555	82 34.80	52 33.40	798.0	4978.08	89.42	0.12
556	82 33.90	52 1.80	715.0	5001.00	87.11	7.10
557	82 31.60	51 47.50	688.0	5017.54	96.22	19.23
558	82 32.40	51 57.80	760.0	4993.97	94.53	9.48
559	82 33.60	52 14.40	736.0	4998.92	91.62	9.26
560	83 46.53	54 7.97	1461.0	4747.17	37.27	-126.22
561	83 56.62	50 32.16	1250.0	4737.67	-40.49	-180.37
562	84 7.70	46 48.90	1290.0	4768.44	-0.86	-145.21
563	82 51.80	53 14.20	1001.0	4902.00	69.45	-42.56
564	82 39.80	51 29.70	1155.0	4866.84	86.29	-42.96
565	82 46.90	53 16.00	941.0	4915.53	66.33	-38.97
566	82 57.20	54 31.50	946.0	4917.00	65.50	-40.36
567	83 3.40	54 56.80	1042.0	4891.88	67.71	-48.90
568	83 34.20	57 21.00	621.0	4950.10	-14.60	-84.10
569	83 34.50	57 18.10	645.0	4944.82	-12.59	-84.76
570	83 34.80	57 14.40	656.0	4942.39	-11.73	-85.14
571	83 35.10	57 10.60	658.0	4943.80	-9.80	-83.43
572	83 35.50	57 7.10	669.0	4943.18	-7.16	-82.03
573	83 35.70	57 3.90	687.0	4939.39	-5.47	-82.35
574	83 36.00	56 59.50	693.0	4938.12	-4.99	-82.54
575	83 36.30	56 56.50	697.0	4947.00	5.02	-72.98
576	82 54.00	53 42.50	935.0	4860.36	6.65	-97.98
577	83 59.10	52 50.90	1441.0	4823.13	103.04	-58.21
578	83 57.00	54 27.90	1483.0	4808.72	102.23	-63.72
579	83 58.10	54 32.20	1448.0	4814.06	96.44	-65.60
580	84 1.90	54 57.40	1291.0	4846.20	79.01	-65.46
581	84 0.20	54 49.50	1379.0	4829.95	90.41	-63.91
582	83 59.60	54 42.10	1420.0	4823.63	96.91	-61.99
583	84 3.20	55 1.10	1267.0	4846.18	71.19	-70.60
584	84 3.90	54 44.10	1233.0	4861.69	76.00	-61.98
585	84 4.00	55 35.90	1537.0	4778.27	86.23	-85.77
586	84 4.90	55 30.50	1250.0	4857.51	76.75	-63.13
587	84 4.10	55 37.20	1223.0	4858.02	69.19	-67.67
588	82 33.30	42 49.68	735.0	4972.32	64.83	-17.42
589	82 17.10	41 42.70	716.0	4953.25	46.30	-33.82
590	82 50.30	54 18.20	763.0	4902.98	-2.36	-87.75
591	82 56.90	53 6.50	1017.0	4834.78	5.28	-108.53
592	83 0.10	52 29.90	1115.0	4815.13	14.66	-110.12
593	83 36.80	44 17.90	1223.0	4814.35	34.32	-102.54
594	83 39.50	43 30.90	1267.0	4791.19	23.82	-117.96
595	83 42.20	42 43.00	1320.0	4768.94	17.01	-130.70
596	83 44.70	41 54.90	1361.0	4785.63	45.51	-106.79
597	83 55.70	38 58.50	1664.0	4704.67	54.37	-131.84
598	83 52.90	39 41.60	1591.0	4723.44	51.54	-126.50
599	83 50.10	40 24.10	1510.0	4750.47	64.51	-114.46
600	85 5.74	65 11.78	1731.0	4788.46	138.64	-55.06
601	85 4.10	64 28.10	1813.0	4766.27	142.14	-60.74
602	85 5.30	64 14.80	1785.0	4784.03	150.97	-48.78
603	85 5.30	64 42.50	1639.0	4813.77	135.72	-47.69
604	85 40.90	69 5.10	1558.0	4825.93	114.30	-60.05
605	85 38.90	68 33.90	1670.0	4801.14	124.47	-62.41
606	85 38.20	69 13.80	1596.0	4806.82	107.51	-71.09
607	85 36.74	68 31.33	1694.0	4789.30	120.52	-69.04
608	85 11.23	64 50.13	1592.0	4817.27	123.23	-54.92
609	85 13.70	64 3.40	1561.0	4764.13	59.91	-114.77
610	85 16.30	63 16.70	1525.0	4764.27	48.39	-122.26
611	85 18.30	62 30.30	1501.0	4758.89	35.04	-132.92
612	85 20.50	61 42.70	1500.0	4726.75	2.36	-165.80
613	85 24.60	60 13.10	1514.0	4772.91	51.53	-117.89
614	85 26.60	59 30.00	1493.0	4745.18	16.85	-150.22
615	85 28.50	58 46.50	1614.0	4715.92	24.42	-156.19
616	85 30.40	58 2.20	1600.0	4724.97	28.71	-150.34
617	85 37.60	54 52.90	1659.0	4686.57	6.81	-178.84
618	85 39.30	53 59.50	1735.0	4663.25	6.51	-187.64
619	85 42.50	52 4.70	1758.0	4643.63	-6.75	-203.47
620	85 43.90	51 5.40	1811.0	4626.79	-7.58	-210.24
621	85 45.30	50 5.70	1804.0	4621.58	-15.25	-217.13
622	85 46.60	49 4.50	1831.0	4599.73	-29.07	-233.97
623	85 0.80	67 21.30	1458.0	4765.42	32.77	-130.38
624	85 2.00	68 27.50	1398.0	4761.15	9.70	-146.74
625	85 3.10	69 33.60	1343.0	4790.89	22.21	-128.08
626	83 37.90	56 11.00	1173.0	4876.64	80.83	-50.43
627	83 39.60	55 43.80	1287.0	4856.39	95.15	-48.67
628	83 40.20	55 24.10	1507.0	4804.74	111.09	-57.55
629	83 43.90	55 15.40	1418.0	4829.58	107.29	-51.39
630	85 2.70	65 45.40	1522.0	4757.79	44.37	-125.95
631	85 4.00	70 40.30	1376.0	4803.86	29.70	-118.68
632	85 5.50	73 3.90	1365.0	4748.04	-14.49	-167.23
633	85 6.20	74 20.90	1391.0	4727.36	-27.33	-182.99
634	85 6.80	75 54.70	1384.0	4728.70	-28.30	-183.18
635	85 7.20	76 56.70	1374.0	4726.43	-33.76	-187.51
636	85 12.70	79 5.50	1392.0	4690.85	-65.19	-220.96
637	85 13.00	80 2.50	1395.0	4684.91	-70.28	-226.39
638	85 13.50	80 58.90	1436.0	4687.79	-64.14	-221.47
639	85 13.70	81 56.20	1434.0	4699.81	-43.54	-204.01
640	84 6.20	56 16.00	1425.0	4815.47	88.23	-71.23
641	84 57.99	67 22.72	1627.0	4788.34	108.50	-73.56
642	84 57.80	67 23.60	1499.0	4823.71	104.48	-63.26
643	84 53.20	67 2.80	1533.0	4821.88	114.36	-57.19
644	84 53.50	67 45.50	1395.0	4849.52	99.39	-56.71
645	84 53.30	69 17.10	1327.0	4864.12	90.78	-56.94
646	83 24.50	55 0.80	1184.0	4864.66	76.78	-55.71
647	83 23.10	55 36.20	1169.0	4871.91	79.90	-50.92
648	83 17.50	55 10.40	1205.0	4866.49	87.52	-47.32
649	83 13.14	54 51.05	1239.0	4847.28	80.33	-58.32
650	83 9.90	55 30.80	1028.0	4907.96	77.13	-37.91

TABLE 2. — Data from gravity reduction program, Camp Neptune, Pensacola Mountains[1]— *Continued*

Sta.	Lat[2]	Long[3]	Elev[4]	Obs G[5]	FAA[6]	BA[7]
651	83 22.30	56 38.90	857.0	4940.10	52.20	-43.70
652	83 25.10	56 59.60	758.0	4968.71	49.33	-35.49
653	83 26.40	56 31.20	787.0	4960.45	49.56	-38.50
654	83 37.80	59 9.50	487.0	5047.32	40.10	-14.39
655	83 42.10	59 2.40	781.0	4979.74	61.73	-25.67
656	84 52.90	62 47.30	1723.0	4793.87	144.97	-47.84
657	84 51.40	64 20.00	1972.0	4735.28	163.49	-57.18
658	84 50.90	64 19.00	2014.0	4743.55	182.70	-42.67
659	84 55.30	65 30.60	1782.0	4775.55	144.18	-55.23
660	84 49.70	65 15.20	2136.0	4704.39	183.58	-55.44
661	84 49.60	65 51.10	2076.0	4713.85	174.59	-57.72
662	84 49.50	67 42.90	1296.0	4875.51	95.96	-49.07
663	84 5.70	56 47.70	1172.0	4891.90	86.85	-44.30
664	84 3.00	56 27.00	1338.0	4851.35	98.30	-51.43
665	84 9.30	56 10.30	1077.0	4880.94	45.51	-75.01
666	83 43.60	56 38.80	877.0	4942.26	53.34	-44.80
667	83 40.00	56 37.80	967.0	4911.50	51.51	-56.70
668	83 16.10	57 37.70	910.0	4979.74	110.34	8.51
669	83 16.20	57 36.60	802.0	5008.28	105.56	15.81
670	83 12.30	57 55.20	984.0	4956.07	110.93	0.82
671	83 6.90	57 35.70	837.0	4993.06	104.44	10.77
672	83 12.10	57 4.60	956.0	4967.63	113.83	6.85
673	83 19.30	58 3.00	700.0	5024.29	89.04	10.71
674	83 20.10	57 26.80	624.0	5024.33	65.38	-4.45
1000	82 51.90	53 22.40	1017.0	4892.40	64.75	-49.06
1001	82 49.50	53 31.60	1072.0	4884.90	75.09	-44.87
1002	82 50.00	53 13.90	1090.0	4874.30	69.86	-52.12
1003	82 46.90	53 16.00	941.0	4915.20	66.00	-39.30
1004	82 46.50	53 45.20	915.0	4916.40	59.33	-43.06
1005	82 25.90	50 33.90	793.0	5025.40	138.68	49.94
1006	82 32.74	47 38.14	715.0	5035.70	92.26	12.25
1007	83 12.10	51 26.50	1464.0	4786.30	89.05	-74.78
1008	83 13.23	51 45.41	1516.0	4783.70	102.07	-67.58
1009	83 16.80	51 58.50	1475.0	4808.20	112.68	-52.38
1010	83 15.70	52 12.20	1417.0	4815.20	102.19	-56.37
1011	83 23.50	53 36.80	1440.0	4804.90	96.26	-64.88
1012	82 39.20	52 58.30	978.0	4922.70	87.83	-21.61
1013	82 37.80	53 30.10	741.0	4978.60	71.22	-11.70
1014	82 36.50	53 33.10	569.0	5011.60	51.70	-11.98
1015	82 34.20	52 41.90	753.0	4993.10	90.80	6.54
1016	82 34.30	52 39.40	777.0	4981.70	86.76	-0.19
1017	82 33.10	52 16.90	816.0	4975.60	93.15	1.84
1018	82 30.20	51 46.90	773.0	4993.00	99.43	11.92
1019	82 33.70	51 44.90	1413.0	4837.60	138.96	-19.21
1020	82 37.80	52 7.60	1216.0	4865.80	104.81	-31.26
1021	82 36.80	53 3.10	961.0	4936.00	96.81	-10.73

[1] Minimum south lat 81°30′, maximum south lat 86°; minimum west long 35°, maximum west long 83°. Gravity base value at Camp Neptune, 982,951.40 mgal. Stations 1—199 observed with LaCoste-Romberg gravimeter G1; stations 500—674 observed with LaCoste-Romberg gravimeter G91; stations 1000—1021 observed with Worden geodetic gravimeter W291.
[2] Latitude, in degrees and minutes.
[3] Longitude, in degrees and minutes.
[4] Surface elevation, in meters.
[5] Observed gravity, in milligals minus 977,000 mgal.
[6] Free-air anomaly, in milligals.
[7] Bouguer anomaly, in milligals. Bouguer anomaly reduced to sea level,assuming a rock density of 2.67 g/cm³. Only values for stations on bedrock were used in compiling plate 1; Bouguer anomaly values at stations used for seismic soundings of ice thickness were reduced as described in text.

☆ U.S. GOVERNMENT PRINTING OFFICE: 1974—543-585/114